

## Speleothems as archives for palaeofire proxies

**Micheline Campbell<sup>1</sup>, Liza McDonough<sup>2</sup>, Pauline Treble<sup>2,1</sup>, Andy Baker<sup>1,2</sup>, Nevena Kosarac<sup>1</sup>, Katie Coleborn<sup>1</sup>, Peter Wynn<sup>3</sup>, Axel K. Schmitt<sup>4</sup>.**

<sup>1</sup>School of Biological, Earth and Environmental Science, UNSW Sydney, Sydney, 2052, Australia

<sup>2</sup>ANSTO, Lucas Heights, Sydney 2234, Australia

<sup>3</sup>Lancaster Environment Centre, Lancaster University, Lancaster, United Kingdom

<sup>4</sup>Institute of Earth Sciences, Universität Heidelberg, 69120 Heidelberg, Germany

Corresponding author: Micheline Campbell (micheline.campbell@unsw.edu.au)

### **Key Points:**

- Wildfires are a serious hazard, and our knowledge is limited by short satellite observational records.
- Cave decorations (speleothems) are a new archive of palaeofire information.
- Both physical and chemical stalagmite features provide palaeofire information

## Abstract

Wildfires affect 40% of the earth's terrestrial biome, but much of our knowledge of wildfire activity is limited to the satellite era. Improved understanding of past fires is necessary to better understand how wildfires might change with future climate change, to understand ecosystem resilience, and to improve data-model comparisons. Environmental proxy archives can extend our knowledge of past fire activity. Speleothems, naturally occurring cave formations, are widely used in palaeoenvironmental research as they are absolutely dateable, occur on every ice-free continent, and include multiple proxies. Recently, speleothems have been shown to record past fire events (McDonough et al., 2022). Here we present a review of this emerging application in speleothem palaeoenvironmental science. We give a concise overview of fire regimes and traditional palaeofire proxies, describe past attempts to use stalagmites to investigate palaeofire, and describe the physical basis through which speleothems can record past fires. We then describe the ideal speleothem sample for palaeofire research and offer a summary of applicable laboratory and statistical methods. Finally, we present four case studies which detail [1] the geochemistry of ash leachates, [2] how sulphur may be a proxy for post fire ecological recovery, [3] how a catastrophic palaeofire was linked to changes in climate and land management, and [4] demonstrate that deep caves can record past fire events. We conclude the paper by suggesting that speleothem  $\delta^{18}\text{O}$  research may need to consider the impact of fire on  $\delta^{18}\text{O}$  values, and outline future research directions.

## Plain Language Summary

Wildfires are a global hazard, and are likely to become larger, more common, and more intense as we feel the effect of climate change. Most of what we know about wildfires come from satellite data, but these datasets are not long enough to fully understand fire behaviour. We can use palaeoclimate data to learn more. Natural cave decorations (stalagmites) form shallow caves have recently been found to include information about fire events. As they grow, stalagmite chemistry changes according to the climate at the time, and recent research has shown that elements from wildfire ash can be incorporated. Here we review the state of the art of knowledge of this new application in palaeofire research. We detail the development of this emerging field, starting with cave dripwater monitoring results, we give an overview of relevant laboratory and statistical methods, and we provide four case studies from southwest Australia investigating ash geochemistry, post-fire changes in sulphur, how intense fires are linked to climate, and how deep cave stalagmites may also record past fires. Longer records of fire activity will help us understand how fire activity might change with climate change, how ecosystems might respond to those changes, and will be used to improve models.

## 1 Introduction

Wildfires are a significant hazard with ~40% of the Earth's terrestrial surface being fire prone, and about ~3% of the terrestrial surface burning each year (Chapin et al., 2011; Giglio et al., 2010). In many areas, instances of dangerous fire weather are increasing (Jones et al., 2022). In northern California and Oregon, the likelihood of extreme autumn fire weather has increased by 40% (Hawkins et al., 2022), and both the frequency and size of wildfires have increased in the western United States (Abatzoglou and Williams, 2016; Iglesias et al., 2022). A long-term increase in both extreme fire weather and fire season length has been observed in parts of Australia (BOM and CSIRO, 2020), and there has been a global increase in the frequency of compound fire weather and meteorological drought events (Richardson et al., 2022). Over the

past three decades, total annual burned area in Australia has increased significantly (Canadell et al., 2021). Additionally, nine of the eleven largest Australian fires on record have occurred since 2000, including 3 of the 4 ‘forest megafires’ observed since 1930 (Canadell et al., 2021). Fire regimes are a function of climate, human activity, and land use (Marlon, 2020). While it can be difficult to ascertain the dominant control, severe fire weather is expected to increase with climate change (Abatzoglou et al., 2019; Di Virgilio et al., 2019). This suggests that it is becoming increasingly important to understand the climatic conditions leading up to catastrophic wildfires to be able to predict and prepare for their occurrence in the future.

Fires play an important role in shaping landscapes (Bowman et al., 2009), and wildfires (or bushfires) have both direct and indirect impacts on the environment and society, including on ecological communities, biogeochemical cycles, hydrology (both surface and sub-surface), erosion rates, and human lives and infrastructure (Bodí et al., 2012; Iglesias et al., 2015; Santín et al., 2012; Woods and Balfour, 2010). The 2018 fires in California, western United States, burned approximately 770 000 ha, or about 2% of California’s land area (Wang et al., 2021). The calculated cost (including capital losses, health costs, and indirect losses) of these fires was between US\$126.1-192.9 billion (or 1.5% of California’s GDP) (Wang et al., 2021). This is similar to the estimated annual cost of bushfires in Australia, which has been given as ~1.3% of Australian GDP (Ashe et al., 2009). The 2019/2020 Australian ‘Black Summer’ bushfires burned 23% of the temperate forests in southeast Australia (an unprecedented event, both nationally and internationally), and were exacerbated by long term anthropogenically-forced climate trends, and at least two modes of climate variability dominating the fire and pre-fire season (Abram et al., 2021). The Black Summer Australian fire season resulted in 33 deaths, more than 3000 houses destroyed, and around 19 million ha burned, including the World Heritage listed Gondwana rainforest which does not normally experience bushfires (Abram et al., 2021; Filkov et al., 2020; Ward et al., 2020). The economic cost (both tangible and intangible) of the 2019/20 fire season has yet to be fully determined, but some estimates have put it in excess of AUD\$200 billion (Read and Denniss, 2020). Two years after the Black Summer bushfires, just 15% of affected Victorian households had rebuilt while after the same period following the catastrophic 2009 ‘Black Saturday’ bushfires, 77% of affected households had rebuilt, were rebuilding, or had bought a new home (May, 2022). A longitudinal study following the Black Saturday bushfires, which had 173 fatalities, found that a small proportion of the population reported post-traumatic stress disorder, depression, psychological distress, and heightened consumption of alcohol years after the event (Bryant et al., 2014).

Our understanding of climate-fire interactions is largely limited to the last few decades, when satellite imagery has been available (Dutta et al., 2016). While the satellite era has enabled us to collect fire data at high spatial and temporal resolutions, it does not capture the full range of natural variability or the transition from Indigenous land management to colonial land management which has occurred since the 17th Century. As a result, proxy studies and, more recently, modelling studies, must be used to fill our gaps in understanding. Earth System Models have only incorporated fire models in the last ~15 years (Li et al., 2013; Liu, 2018; Teixeira et al., 2021), and improvements are needed to resolve vegetation feedbacks and incorporate anthropogenic activity (via fire suppression or promotion) to improve model performance (Brücher et al., 2014; Hanan et al., 2021; Kehrwald et al., 2016). The development of the Global Charcoal Database (now Global Paleofire Database; <https://www.paleofire.org/index.php>) has been a key step in enabling hypothesis testing, evaluation of climate-fire interactions, and the development of composite charcoal proxy records which can reconstruct fire activity with

improved signal to noise ratios (Fohlmeister, 2012; Power et al., 2010). However, some regions (e.g., Africa, Australia, South America) remain under-researched, with poor data density in the database. This leaves a large knowledge gap in the palaeofire community which may be addressed by the development of new proxy archives. Fire proxy archives such as sedimentary charcoal, tree scars, and chemical signals in ice cores have been used to extend the observational record and better understand fire regimes at local to continental scales. Existing proxy archives such as tree scars, sedimentary charcoal, ice cores, and historical records may be biased by survivorship (tree scars), have decadal or longer resolutions (sedimentary charcoal), be resolved only at continental or hemispheric scales (ice cores), and may be too short to capture the full range of natural variability (historical records). Speleothems, secondary cave formations, offer a new archive for fire proxy data, with some advantages over traditional fire proxy archives. They may be absolutely dated using radiometric techniques, have high temporal resolutions, and incorporate a wide range of proxies, allowing for coupled records of climate and fire. Additionally, speleothems may fill key geographical gaps where few tree ring and sediment core records have been developed (e.g., southwest Australia).

Here, we present an overview of the processes which control fire regimes and associated investigative methods, including satellite products and proxy data (Sections 2 and 3). In Section 4, we describe recent advances in the development of speleothems as proxy archives for fire research, and provide an overview of the relevant proxies. We include a summary of the field, laboratory, and statistical methods relevant to constructing speleothem-based palaeofire records (Section 5). In Section 6 we present four case studies that demonstrate how: [1] speleothem trace metals may be used to identify fire events and intensity, [2] sulphate isotopes and speleothem sulphur can be used to understand post-fire recovery, [3] speleothem fabric can be used to identify intense fire events, and [4] the influence of cave depth on the preservation of fire in the speleothem record. The development of speleothems as fire proxy archives is of global significance, as speleothems are found on all continents bar Antarctica, and are already widely used by the palaeoenvironmental community. In this review, we build on recent research in Australia, but the information and case studies presented here identify the processes that will inform proxy response worldwide.

## 2 Understanding fire regimes

Fire regimes are a function of climate, human activity, and vegetation composition, and may be non-stationary in time and space (Hantson et al., 2016; Marlon, 2020). Fire reconstructions can now be linked to known climate shifts, including the Medieval Climate Anomaly (where warm and dry conditions in North America were accompanied by increased burning, including the highest fire activity in two 3000 year records (Marlon et al., 2012; Swetnam et al., 2009)), and the Little Ice Age, when cooler temperatures in western North America were accompanied by the lowest biomass burning in the late Holocene (Marlon et al., 2012). The relationship between climate and fire is not always geographically consistent. Antecedent drought conditions generally underpin extreme fire years in the northwestern United States (Gedalof et al., 2005), but in the semi-arid regions of Australia high annual precipitation in the preceding year is a key precursor to large fire events due to enhanced fuel loads (van Etten et al., 2021). While global and continental analyses have suggested that climate has been the primary control on fire regimes (Mooney et al., 2011; Pechony and Shindell, 2010; Power et al., 2008), at the regional scale, there is ample evidence that humans have used fire for protection, hunting and gathering, and land management for tens of thousands of years (Fletcher et al.,

2021a; Mariani et al., 2022). This suggests that so-called ‘natural’ fire regimes are modified by human activity, at least at sub-continental scales. Palaeoenvironmental records support this, demonstrated by upticks in fire frequency well-linked to human activity (Fletcher et al., 2021a; Haberle and David, 2004; McDonough et al., 2022; McWethy et al., 2010; Rehn et al., 2021; Wang et al., 2013). Similarly, the more-recent transition from Indigenous (fire-promoting) to colonial (fire suppressing) land management practices has seen associated changes in fire regime (Fletcher et al., 2021a, 2021b; McDonough et al., 2022).

Improved knowledge of past fire regimes and associated past climate will enable us to; [1] better understand how wildfires might change with future climate change, [2] better understand ecosystem resilience, which will inform land management practices, and [3] improve data-model comparisons. For example, long records of fire severity and frequency can provide baseline data for characterising long-term variability. This will enable us to determine the departure from this baseline, which will itself aid attribution studies on the impact of climate change. Current ecosystems have evolved over tens of thousands of years of Indigenous land management practices. Being able to better understand the impact of these land management practices on past fire regimes will enable better decision making about how ecosystems should be managed to optimise their resilience. For example, Mariani et al. (2022) showed that the disruption of cultural burning practices has changed ecosystems and led to recent unprecedented wildfires. Observational data-model comparisons have been used to quantify emissions and fire intensity, but satellite datasets are short, and do not capture the full range of climate variability (Hantson et al., 2016; van Marle et al., 2017). Using long-duration proxy data allows for better understanding of the full range of fire regime variability, and can be used to validate climate simulations under vastly different conditions to the present (Hantson et al., 2016; Harrison et al., 2014; Schmidt et al., 2014).

### 3 Palaeofires

Prior to the satellite era, fire documentation is poor. While historical records may document fire frequency and intensity, there is high uncertainty and variability around geographic and temporal extents. Fire records from archives which form with annual laminae, and which have extension rates high enough such that analytical requirements are met, may enable high-resolution reconstructions (Marlon, 2020). To date, such records have been sourced from archives including ice cores, fire-scarred trees, and charcoal preserved in sediment cores. Each of these archives have their own strengths, weaknesses, relevant temporal and spatial scales, and ideal applications (see Table 1 and Figure 1). While these traditional fire proxy archives have been extensively used to reconstruct past fire behaviour, speleothems are a novel fire archive with the potential to develop high resolution, absolutely dated coupled climate-fire records. This is especially exciting for regions such as southwest Australia where there are relatively few published tree ring and sediment palaeofire records, but a large network of caves which have already produced stalagmites suitable for palaeoclimate and palaeofire research (McDonough et al., 2022).

**Table 1** Established sources of fire information, and their properties

| Proxy Archive | Proxy/ies | Strengths | Weaknesses | Example references |
|---------------|-----------|-----------|------------|--------------------|
|---------------|-----------|-----------|------------|--------------------|

|                                     |   |  |  |  |
|-------------------------------------|---|--|--|--|
| <b>Marine, lake, and peat cores</b> | Charcoal (macro and micro)  | Cost-effective collection, analyses and storage; Age measurements directly on charcoal; Widely preserved; global database allows for regional reconstructions; Potential for coupled fire-climate reconstructions using pollen from the same core. | May be biased towards large and intense fires; Usually decadal or lower resolution; May be discontinuous due to erosion or if peat burns; Charcoal quantity not related to fire extent or intensity limiting to qualitative interpretation; Reconstructions are unitless due to standardization. | Marlon, 2020; van Marle et al., 2017; Whitlock and Larsen, 2001  |
| <b>Ice cores</b>                    | Biomarkers, aerosols, electrical resistivity, isotopes, and trace elements. | Potential for coupled climate-fire records; May be long-duration and resolvable at seasonal scales; Large-scale (regional to hemispheric) overview of fire activity.   | Expensive to collect, store, and analyse; Cannot be resolved at sub-continental scales; Require understanding of large scale atmospheric transport processes for interpretation.   | Bhattacharai et al., 2019; Grieman et al., 2018; Legrand et al., 2016; Marlon, 2020; McConnell et al., 2007; Rubino et al., 2016 |
| <b>Trees</b>                        | Fire scars and stand establishment dates.                                   | Precisely dateable; Coupled climate-fire records; Cost-effective sample collection, storage, and analysis.   | Survival and preservation bias; Highly local records; Cannot reconstruct fire intensity.   | McBride, 1983; O'Donnell et al., 2010; Reifsnyder et al., 1967   |
| <b>Historical observations</b>      | Weather reports, journals, etc.   | May be quantitative (e.g. fire extent); Digitisation has encouraged recovery of old records.   | Relatively short duration; Highly local; May be discontinuous; Often qualitative.  | (Gruell, 1985; Lucas, 2010; Stamou et al., 2016)   |

Marine, lake, and peat cores incorporate sedimentary charcoal as they accumulate. Sedimentary charcoal research has informed the bulk of palaeofire knowledge, largely underpinned by the development of the Global Charcoal Database (now Global Paleofire Database), a crowd-sourced public-access database of sedimentary fire proxies (Brücher et al., 2014; Marlon et al., 2016; Molinari et al., 2021, 2013; van Marle et al., 2017). Sediment cores can be retrieved from lakes, peat bogs, ocean floors, and alluvial fans, and both macro- and micro-charcoal can be used as fire proxies (Marlon, 2020; Whitlock and Larsen, 2001). Sedimentary charcoal records generally have approximately decadal temporal resolutions, although annual resolution may be achieved (Vachula et al., 2018). Sedimentary charcoal records can be biased towards larger and more intense fires as there is a bias in the transport and preservation of charcoal from small events, although this may be overcome by analysing only macro charcoal, or accounting for the source area by looking at the distribution of charcoal sizes (Mariani et al., 2016; Vachula et al., 2018). While peaks in charcoal concentrations are not empirically linked to fire intensity, other approaches such as Attenuated Total Reflectance

Fourier Transform Infrared spectroscopy have been used to characterise the structure and carbonization temperatures of charcoals (Constantine et al., 2021; Gosling et al., 2019), although burn temperature is just one aspect of fire intensity (Keeley, 2009).

Fire proxies found in ice cores include biomarkers (e.g. levoglucosan, vanillic acid), aerosols (e.g., black carbon), isotopes (e.g.,  $\delta^{13}\text{C}$ -CH<sub>4</sub>), electrical resistivity, and trace elements and nutrients (e.g. potassium, nitrate and nitrite) (Rubino et al., 2016). Due to atmospheric processes, ice cores record an attenuated signal which cannot usually be linked to individual events, although their annual laminae do allow changes in fire emissions at a regional to continental scale to be precisely dated (Marlon, 2020; van Marle et al., 2017). Interpretation of ice core fire proxy data requires an understanding of atmospheric processes and transport, as they are remote proxies which give an overview of large scale changes in biomass burning (Battistel et al., 2018; Marlon, 2020). Nonetheless, ice core fire records have successfully been applied to investigate past fire activity (Battistel et al., 2018; Eichler et al., 2011; Nicewonger et al., 2020), and links to anthropogenic land clearing (Zennaro et al., 2015).

Trees record local fire events with fire scars, which can be precisely dated by counting tree rings. Annual growth rings mean that fire scar records have annual temporal resolutions, although their spatial resolution is highly localised. As scar size is not linked to fire intensity (and old scars may be enlarged by subsequent fires), tree scars only record fire frequency (McBride, 1983; Reifsnyder et al., 1967). Additionally, fire scar records are impacted by several biases, including survivorship bias which is related to tree age and fire intensity, and bark thickness bias as a result of thicker bark being less likely to scar, so as trees age they record fewer fire events (McBride, 1983; Reifsnyder et al., 1967). In environments where post-fire tree mortality is high, stand establishment (or replacement) dates may be used as a proxy for the last stand-replacing fire (Brown et al., 1999). Drawbacks of this approach are that creating a timeseries is difficult, lags in re-establishment are unknown, and chest-height samples may not include all growth rings (although this can be resolved by sampling at lower heights) (O'Donnell et al., 2010).

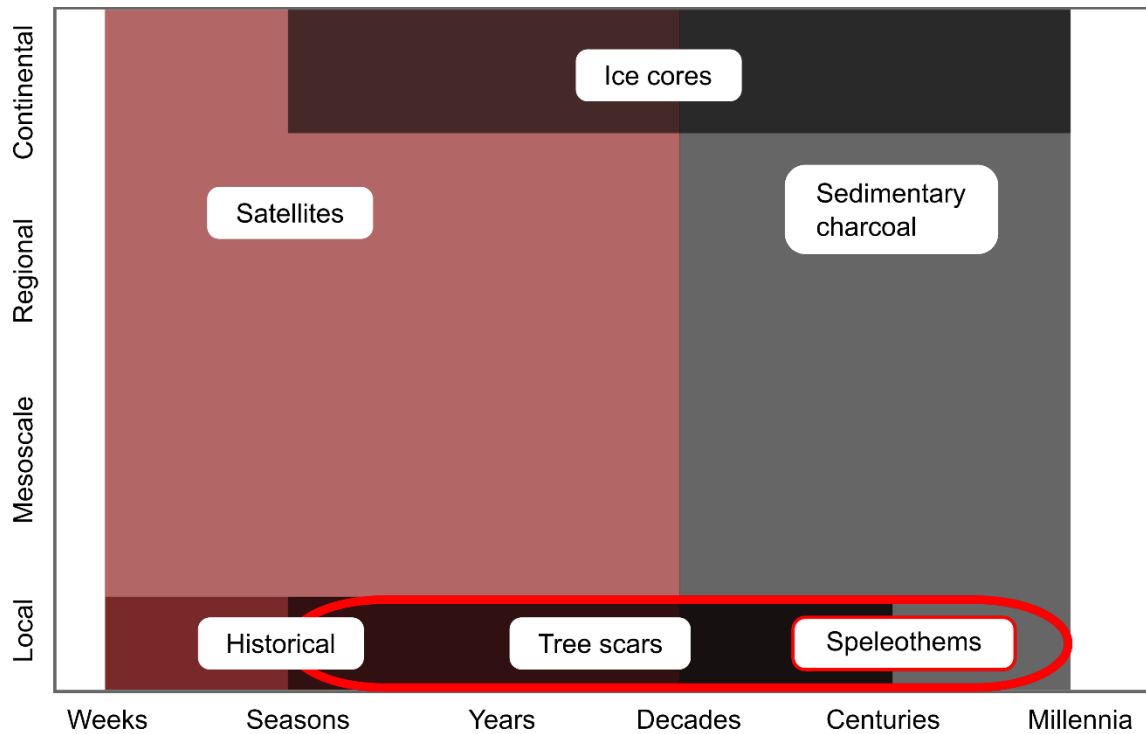


**Figure 1** Proxy and observational sources of fire data and their spatial and temporal resolutions. Observational sources are maroon, proxies are black. Potential temporal and spatial resolution of speleothems is shown as a red box. Opacity for each archive except speleothems is 60%, so dark regions indicate where archives overlap. For example, historical records are mainly local, but cover periods of time from weeks to centuries. Adapted from Kehrwald et al. (2016).

#### 4 Speleothems as palaeoenvironmental archives

Calcareous speleothems (stalagmites, stalactites, and flowstones) are naturally occurring formations which grow in caves due to the dissolution of limestone and subsequent precipitation of calcium carbonate. Stalagmites are excellent natural archives for palaeoenvironmental research as they are absolutely and precisely datable, can produce long, continuous records, include multiple proxies, and their links to surface hydroclimate and utility as palaeoclimate archives are well established.

Speleothems can be absolutely dated using radiometric techniques. Typically uranium-series techniques are preferred, with radiocarbon dating used where uranium-series dating is complicated by the inclusion of detrital thorium or low uranium concentrations (Hua et al., 2012; Zhao et al., 2009). In climates with high seasonality such as Mediterranean climates with distinct summer-winter seasonality speleothems form clear physical and chemical annual laminae (Baker et al., 2021). Where speleothems were sampled while actively growing, these annual laminae can be counted to develop highly accurate and precise annual chronologies with minimal error (Faraji et al., 2021; McDonough et al., 2022; Nagra et al., 2017).

Speleothems have been widely used to reconstruct regional temperature, precipitation and larger-scale atmospheric processes such as variability in the Asian Monsoon, and the El Niño-Southern Oscillation (Chen et al., 2016; Cheng et al., 2016). Speleothem proxy records which are both long and of very high resolution (seasonal or better) provide an almost-unique opportunity



to reconstruct climate at human-relevant timescales, that is, seasonal to decadal fluctuations which have potential to influence human wellbeing and behaviour. Such speleothems have been found in the Levant, and have provided insight into the interplay between climate and early human migration through the Middle East during the Last Interglacial. Orland et al. (2019) undertook a data-model comparison of seasonal speleothem  $\delta^{18}\text{O}$  and simulated monthly precipitation  $\delta^{18}\text{O}$  from comparative atmospheric model runs of precession-high and precession-low northern hemisphere seasonality. Using Secondary Ion Mass Spectrometry, with replicates along each lamina, they were able to collect high-resolution (10  $\mu\text{m}$  spots) in situ calcite  $\delta^{18}\text{O}$  (Orland et al., 2019). Their results tied periods of precession-high northern hemisphere seasonality with the appearance of early hominin fossils in the Levant (Herskovitz et al., 2018; Orland et al., 2019). This demonstrates how high-resolution palaeoclimate records can provide insight into past human-environment interactions.

Datasets with multiple proxies allow for greater certainty in the interpretation of palaeoenvironmental records and for the use of multivariate statistical methods. Proxies derived from speleothems include oxygen and carbon stable isotopes, trace elements and metals, fluorescence, organic matter content, pollen, organic macromolecules, and growth rate. While stable isotopes are the most widely used speleothem proxy, in recent decades trace elements and physical properties such as growth rate and changes in speleothem fabric have become more commonly applied, (Frisia, 2014; McDonough et al., 2022; Orland et al., 2014; Treble et al., 2005). As a mature discipline, the links between speleothem geochemistry and regional hydroclimate are relatively well-constrained. Speleothem  $\delta^{18}\text{O}$  is controlled by precipitation  $\delta^{18}\text{O}$  and hydrological processes in the soil, epikarst, and cave system (Bradley et al., 2010; Lachniet, 2009). Karst flowpaths play an important role in often amplifying the drip  $\delta^{18}\text{O}$  response to climate and have been shown to be ubiquitous in a global analysis (Treble et al., 2022) and cave monitoring can assist with quantifying this.

Seasonal variations in trace elements (such as Sr/Ca), combined with the development of high-resolution, non- and minimally-destructive analytical techniques, mean that trace elements are becoming more commonly used in speleothem palaeoenvironmental research. Trace element ratios are controlled by atmospheric inputs, biological processes in vegetation and soil, hydrological processes in the karst and epikarst, crystal growth processes, and secondary alteration (Fairchild and Treble, 2009). Trace element variations have been used to investigate drought onset and duration, normally via the Mg/Ca ratio and its association with prior calcite precipitation, where precipitation of calcite within the flow path ‘upstream’ of the drip point during drier conditions results in higher ratios of magnesium to calcium (Fairchild and Treble, 2009; Griffiths et al., 2020). Subaqueous speleothem Mg/Ca has also been used as a palaeotemperature proxy (Drysdales et al., 2020). Sr/Ca is also affected by prior calcite precipitation and may be used as an aridity proxy, although analysis of strontium isotopes has shown that aeolian inputs can alter the signal (Goede et al., 1998). However, a correlation between Sr/Ca and Mg/Ca increases the confidence that variations are hydrological. Beyond palaeoenvironmental applications, seasonal changes in Sr/Ca may be used to develop precise annual speleothem chronologies (e.g. Nagra et al., 2017). It has been demonstrated that trace metals are transported in infiltrating karst waters as both particulates and colloids with organic matter, with dripwater-metal ratios closely associated with NICA-Donnan n1 humic binding affinity ratios (Hartland et al., 2012). Hartland et al. (2012) also showed that transport was partitioned by size, with all sizes more easily transported under high-flow conditions (when fractures are activated), while during low-flows particulates and small colloids decoupled.

Speleothem sulphur and sulphate concentrations and isotopes have been used to investigate industrial pollution and past volcanic activity, and sulphate isotopes enable pollution provenance as well as emissions quantification (Borsato et al., 2015; Wynn et al., 2010, 2008).

#### 4.1 Previous attempts at using speleothems for palaeofire research

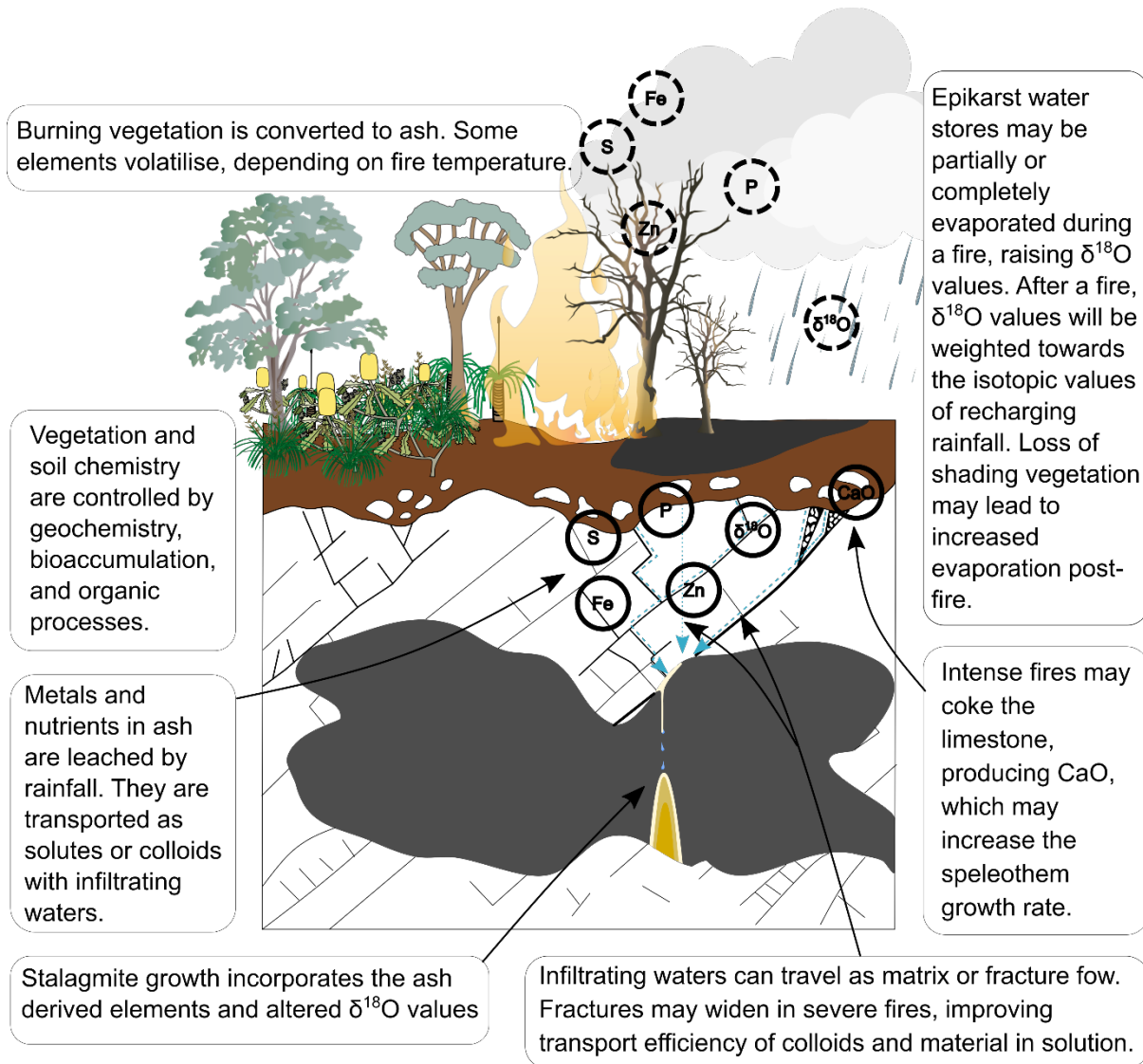
Black laminae and black cave deposits have been reported in stalagmites from Slovakia (Gradziński et al., 2007), the United States (Benington et al., 1962), Slovenia (Šebela et al., 2017, 2015), and Australia (Dredge, 2014; Spate and Ward, 1979; Webb et al., 2014). While black deposits are generally attributed to guano, fossil fuel combustion, cooking fires, and torches (Benington et al., 1962; Gradziński et al., 2003; Kaal et al., 2021; Šebela et al., 2015; Zupančič et al., 2011), in Australia and Slovakia it has been suggested that these black deposits are records of bushfires. Analyses conducted in the 1970s suggested that black layers at Yarrangobilly Caves, Australia, were comprised of silica and carbon, and that a bushfire origin was reasonable (Spate and Ward, 1979). However, subsequent research at Yarrangobilly found no evidence of charcoal in black cave residues, and comparisons of growth-rate-weighted polycyclic aromatic hydrocarbon concentrations in black and white calcite samples showed no difference (Dredge, 2014). A multi-proxy study of a flowstone from the same cave system concluded that the black layers were due to high concentrations of humic substances delivered during intense wet periods (Webb et al., 2014). These studies both suggest that speleothem colour at Yarrangobilly is unlikely to be a direct outcome of wildfire, with bacterial melanisation, bioaccumulation of iron and manganese oxides proposed as alternative mechanisms for calcite colouration (Dredge, 2014; Gázquez et al., 2011). Slovenian caves feature similar black deposits, which have been attributed to forest fires through comparison between calcite  $\delta^{13}\text{C}$  and  $\delta^{13}\text{C}$  of charcoal in soil, visualisation with scanning electron microscopy/energy dispersive spectroscopy, and quantification of organic carbon (Šebela et al., 2017). The authors acknowledged that transmission of particulates into the Postojna and Predjama Caves would be more likely to occur during winter when cool air is able to settle into the relatively warmer cave (Šebela et al., 2017). Following this, in regions where the wildfire season occurs during summer and outside temperatures are higher than cave temperatures, it is unlikely that smoke particulate would be able to enter and settle in caves due to the temperature gradient suppressing the entry of outside air masses when external temperature exceeds cave temperature. This temperature gradient could be further enhanced by the fire locally influencing air temperature. While black residue in caves may record nearby bushfires, it is likely that this only occurs under specific circumstances (e.g., a cave with chimney ventilation in the side of a valley) likely explaining why black residue is so rarely reported. With polycyclic aromatic hydrocarbons just as common in black calcite as white calcite (Dredge, 2014), any palaeofire reconstruction built on calcite colouration alone is likely to be erroneous. Where black residues have been more strongly linked to fire activity, (that is, in Slovenia; Šebela et al., 2017), cave atmospheric processes may limit the recording of fire to cooler season fire activity, reducing its utility to investigate past fire regimes.

#### 4.2 Developments in high-resolution fire proxies in speleothems

In recent years, publications have reported that fire and post-fire responses have been directly observed in cave monitoring studies highlighting the possibility of constructing fire records using speleothems (Bian et al., 2019; Coleborn et al., 2019, 2018; Nagra et al., 2016; Treble et al., 2016). Importantly, the results of these studies showed that speleothem-based

palaeofire records could be achieved using a subset of typically measured variables such as speleothem stable isotopes, discharge rate, and trace elements and nutrients. This has subsequently been confirmed by McDonough et al. (2022) who showed in a young speleothem that: [1] the stalagmite recorded a response to all known fire events that had burnt over the cave in the four decades between 1966 and 2005; and [2] that this information could be applied to reconstruct palaeofires. Primarily, these studies have shown that fire events may be recorded by speleothems through the loss of stored shallow water and loss of vegetation, the infiltration and incorporation of ash- and soil-derived elements, changes in calcite fabric induced by the influx of foreign ions and particles and changes in speleothem extension rate owing to changes in carbonate chemistry resulting from heating of the limestone and impact on soil CO<sub>2</sub>. Critically, these dripwater monitoring studies have shown that the proxy response is modulated by fire severity and cave depth (Figure 3). The proxy response is present in the largest number of proxies in shallow caves which experienced more severe fires (Bian et al., 2019; Nagra et al., 2016). Deeper caves which also experienced less severe fires showed a more muted (Treble et al., 2016) or entirely absent (Coleborn et al., 2019, 2018) proxy response. Here we have produced two new figures to summarise these studies. Figure 2 shows a conceptual illustration of the proxies and processes identified in these studies and Figure 3 shows which proxies showed a response to fire in each cave monitoring study, ordered by cave depth. In the remainder of Section 4, we expand on these proxies and the relevant processes from these and other studies.

366



367

368 **Figure 2** Conceptual model of processes underpinning the production, transport, and  
 369 incorporation of known speleothem fire proxies.

370 Fire impacts have been well-documented in surface hydrology (predominantly in non-  
 371 karst environments), with reported downstream increases in nitrate, phosphate, turbidity, and  
 372 decreases in dissolved oxygen and pH (Dahm et al., 2015; Reale et al., 2015; Sherson et al.,  
 373 2015). In surface waters, erosion (a primary driver of changes to hydrochemistry) may continue  
 374 for many years following a fire event, particularly if vegetation recovery is slow and there is a  
 375 delay in extreme precipitation events (Shakesby, 2011). Ash chemical composition is well-  
 376 understood, and has been found to vary with underlying geology, vegetation composition, and  
 377 fire intensity (Alriksson and Eriksson, 1998; Bodí et al., 2014; Cerrato et al., 2016; Khanna et al.,  
 378 1994). Chemical concentrations in ash may be higher than in vegetation, suggesting  
 379 bioaccumulation and concentration of elements (Cerrato et al., 2016).

In the highly porous karst landscape, dissolution and colloidal transport of a large proportion of ash-derived elements is likely to occur via infiltration to the epikarst and groundwater rather than via surface flow to rivers and streams. This is consistent with the colloidal and dissolved transport of common trace elements through karst (Borsato et al., 2007). Transport of ash-derived elements is a function of their solubility (or adsorption to colloidal particulates and minerals), and may be confounded by losses through mineralisation or biological uptake (Khanna et al., 1994; Treble et al., 2016). The geological and species controls on ash chemistry, as well as variable rates of dissolution, transport, mineralisation, and biological uptake suggest that it may not be possible to quantifiably compare changes in ash chemistry between regions.

The mechanisms by which a speleothem may incorporate the fire signal are broadly separated into physical and chemical processes. Physical processes include modifying the volume of stored water by evaporation, fracturing of host rock, increased soil hydrophobicity and preferential flow, conversion of limestone to lime, and changes to soil CO<sub>2</sub> production. Chemical processes include the introduction and transport of ash-derived trace elements and metals and the impact of limestone coking on CaO production and speleothem extension rate.

#### 4.2.1 Impact on hydrology

Increased evaporation can impact the  $\delta^{18}\text{O}$  signal depending on the relative loss of shallow stored water in the soil or epikarst zone and subsequent recharge events. Surface heating from fire may directly evaporate stored water during a fire event, and prolonged evaporation post-fire may occur due to reduced overstorey and ground cover (loss of shading) (Bian et al., 2019; Nagra et al., 2016). While transpiration can be elevated in post-fire regrowth (Buckley et al., 2012), transpiration does not result in fractionation of soil water. The post-fire  $\delta^{18}\text{O}$  response in cave dripwaters has been shown to vary, with both higher and lower values observed (Figure 3). Following a bushfire over a shallow forested cave in southwest Australia, Nagra et al. (2016) found an increase in dripwater  $\delta^{18}\text{O}$  values attributed to increased evaporation because of loss of canopy cover and reduced albedo (Nagra et al., 2016). Conversely, Bian et al., (2019) found that  $\delta^{18}\text{O}$  declined following an experimental fire over a shallow cave in southeast Australia. They attributed this to the complete evaporation of stored soil/epikarst water during the fire, followed by recharge by an isotopically low precipitation event (Bian et al., 2019). They also noted that reduced capillarity and increased preferential flow in the soil may have further assisted post-fire recharge (Bian et al., 2019). In the same cave monitored by Nagra et al. (2016), an increase in stalagmite  $\delta^{18}\text{O}$  in the year following a reconstructed fire event in 1897 CE was noted and this was attributed to increased evaporation as seen in Nagra et al. (2016) (McDonough et al., 2022). A subsequent shift to lower  $\delta^{18}\text{O}$  values in the stalagmite record was interpreted as a return to wetter conditions with the caveat that a change in hydrology due to fracturing and preferential flow may have amplified the shift in calcite  $\delta^{18}\text{O}$  values (McDonough et al., 2022).

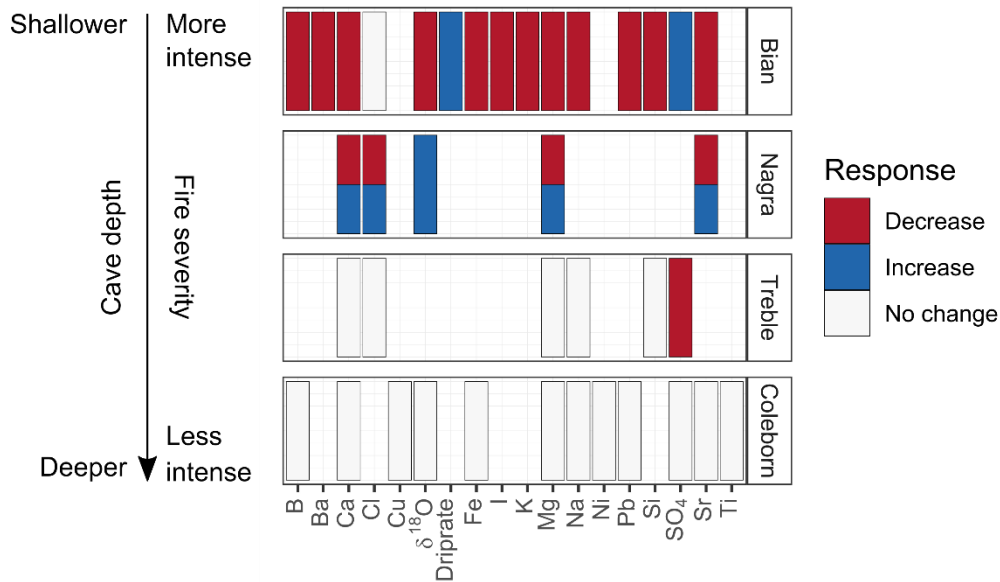


**Figure 3** Published proxy responses to fire events in dripwater (Bian et al., 2019; Coleborn et al., 2018; Nagra et al., 2016; Treble et al., 2016). Red indicates a post-fire decrease in a proxy, blue indicates a post-fire increase in a proxy, and white shows that no change was recorded. Results are presented in order of cave depth and fire severity, with the shallowest cave and most severe fire at the top of the figure, and the deepest cave and least severe fire at the bottom of the figure.

Fracturing of host rock and increased soil hydrophobicity have been both observed and inferred in the  $\delta^{18}\text{O}$ , trace element and organic matter responses to fire (Bian et al., 2019; McDonough et al., 2022; Nagra et al., 2016). Limestone structure can be impacted by temperatures  $>500^\circ\text{C}$  (base temperatures in a large fire can exceed  $1000^\circ\text{C}$ ), with heating and cooling leading to fracturing or widening of fractures in the epikarst (Meng et al., 2020; Wu and Wang, 2012). Bushfires can also enhance soil hydrophobicity. In an experimental trial on eucalypt forest, Granged et al. (2011) found that post-fire water repellence was greatest after a low-intensity fire, and that soil water repellence persisted for some months. Medium and high-intensity fires completely destroyed soil water repellence, which was attributed to a large reduction in soil organic matter after peak temperatures of  $317$  and  $525^\circ\text{C}$  (Granged et al., 2011). Increased fracturing and soil water repellence can both result in increased preferential flow and so alter vadose zone hydrology, resulting in more direct connectivity between the surface and the cave. Bian et al. (2019) interpreted a post-fire negative excursion in  $\delta^{18}\text{O}$  to isotopically heavier precipitation being rapidly transported to the cave due to an increase in preferential flow. They noted that dripwater isotopic composition returned to an integrated mean after  $\sim 6$  months as soil water stores were replaced (Bian et al., 2019). McDonough et al. (2022) attributed a rapid increase in organic matter concentration to enhanced meso- and macro-porosity of the bedrock as a result of limestone heating, and increased flushing of soil organic matter through the bedrock. This is consistent with field trials which have shown losses of organic matter from the soil surface associated with soil water repellence (Lowe et al., 2021). In places where soil water repellence is already high (such as in the sandy soils of Western Australia), exacerbation of soil water repellence by moderate fire and destruction of non-wetting soils by severe fire may be a key consideration in separating severe and moderate fire events in the proxy record. Beyond fracturing and hydrophobicity, heating of limestone can also result in localised

lime formation. This leads to enhanced supersaturation as that lime is preferentially dissolved by infiltrating waters, resulting in a higher speleothem extension rate (Hartland et al., 2010; Kemperl and Maček, 2009; Moropoulou et al., 2001). This phenomenon was observed by McDonough et al. (2022), when extension rate increases followed a large inferred palaeo-fire event.

#### 4.2.2 Impact on soil microbiology

Soil CO<sub>2</sub> is a key driver of stalagmite formation, as it is a major control of dissolution in karst environments (Dreybrodt, 1999). Plant respiration and microbial activity produce soil CO<sub>2</sub> with partial pressures 1—3 orders of magnitude greater than that of the atmosphere (Appelo et al., 2005). Fallen precipitation absorbs this CO<sub>2</sub>, becoming mildly acidic. This mildly acidic water then dissolves the parent rock as it infiltrates. Only when this infiltrating water encounters a region of lower partial pressure of CO<sub>2</sub> will CO<sub>2</sub> degas and calcite precipitate (Fairchild and Baker, 2012). When vegetation and microbes are destroyed by fire, soil CO<sub>2</sub> concentrations are suppressed. The impact of fire on total soil respiration is a function of fire severity, vegetation, microbe age and species composition, fire regime, and soil moisture (Bárcenas-Moreno and Bååth, 2009; Certini, 2005; Gongalsky et al., 2012; Arturo J.P. Granged et al., 2011; Arturo J. P. Granged et al., 2011; Hart et al., 2005; Jenkins and Adams, 2010; Neary et al., 1999; Pharo et al., 2013; Uribe et al., 2013; Zedler, 2007). Coleborn et al. (2016) investigated the long-term response of karst soil CO<sub>2</sub> in woodland and grassland, and subalpine forest environments. They found that soil CO<sub>2</sub> concentrations take >5 years to return to pre-fire levels in a woodland and grassland landscape, and >10 years to recover in a subalpine forest, and that recovery was associated with the vegetation recovery rate (Coleborn et al., 2016b). It follows that disruption of soil microbiology and CO<sub>2</sub> abundance due to fire may impact speleothem growth rate,  $\delta^{13}\text{C}$ , and  $\delta^{14}\text{C}$ , although further research is required to quantify this phenomenon.

#### 4.2.3 Impact on speleothem fabric

Speleothem fabric refers to the configuration of calcite or aragonite crystals forming the speleothem and is characterised by their size, orientation, arrangement, preservation, and intra-crystalline porosity. These are controlled by cave parameters such as dripwater flow type and variability, cave temperature, calcium saturation, solute chemistry, foreign particles and biological communities (Fairchild and Baker, 2012; Frisia and Borsato, 2010). Hence, speleothem fabric has been used to infer hydrology and post-depositional processes (Fairchild and Baker, 2012). Repeated fabric patterns have been observed in laminated speleothems from sites with high climatic seasonality, and likely reflects seasonal changes in dripwater composition (Frisia and Borsato, 2010). Speleothems dominated by low-porosity fabrics (e.g. columnar fabrics with low visible intercrystalline porosity; Frisia, 2014), are generally favoured for palaeofire reconstructions as these fabrics are more suitable for high resolution in situ techniques such as X-ray Fluorescence Microscopy XFM and Synchrotron micro X-ray fluorescence (S- $\mu\text{XRF}$ ), laser ablation inductively coupled plasma mass spectrometry (LA-ICP-MS) and secondary ionisation mass spectrometry (SIMS). See Frisia (2014) for further description of speleothem fabric types.

Analysis of speleothem fabric has been shown to be a useful tool for identifying palaeofires. McDonough et al. (2022) logged speleothem fabric following the schema of Frisia (2014) and found that a large palaeofire in the record (see also Section 6.3) coincided with a

micro-hiatus in growth defined by optical continuity in crystal growth, no dissolution of crystal tips, and no evidence of renucleation. Following this micro-hiatus (after the fire event), crystal fabric became more porous with acute crystal tips (McDonough et al., 2022). They determined this was due to an influx of impurities, which initially occluded growth, and then temporarily poisoned growth sites at calcite surfaces over the next six years, resulting in higher porosity (McDonough et al., 2022).

#### 4.2.4 Impact on inorganic proxies

Post-fire cave dripwater monitoring showed that dripwater geochemistry can be impacted by fires. Post-fire responses in dripwater  $\delta^{18}\text{O}$  values and sulphate concentrations are covered in Section 4.2.1 and 6.2, respectively. Here, we describe post-fire changes in inorganic proxies such as dripwater solutes that may be ultimately incorporated as trace metals in speleothems that are also summarised in Figure 3.

Dripwater monitoring following an intense fire in 2005 over Yonderup Cave (~4 m below ground level), southwest Australia, showed that the response of water soluble ions (chlorine, calcium, magnesium, strontium) differed between two monitored drip sites in the cave, with ions decreasing at Site 1a, and increasing at Site 2a (Figure 3; Nagra et al., 2016). Solute concentration through increased evaporation was suggested as the reason for increased post-fire concentrations at Site 2a, with declining solutes at Site 1a attributed to reduced transpiration and a gradual return to base concentrations following a pulse of ash-derived solutes (Nagra et al., 2016).

To further test the hypothesis that dripwater geochemistry is influenced by fires, experimental burns were carried out over two caves in southeast Australia (Bian et al., 2019; Coleborn et al., 2018). Following a low intensity controlled burn over South Glory Cave, a deep (~40 m) cave in southeast Australia, no significant change in dripwater chemistry was noted (Coleborn et al., 2019, 2018). Conversely, a high intensity prescribed burn over Wildman's Cave in southeast Australia (~1 m below ground surface) led to declines in a suite of elements (boron, barium, calcium, iron, iodine, potassium, magnesium, sodium, silicon, and strontium) and an increase in dripwater sulphate (Bian et al., 2019). Flow to the shallow Wildman's Cave is entirely dominated by fractures, and the karst has no remaining matrix porosity (Bian et al., 2019; Osborne, 1993). This may explain the clear and significant post-fire change in dripwater chemistry as the signal is transported rapidly with minimal opportunity for mixing. Conversely, South Glory Cave karst (Yarrangobilly Karst) is also highly fractured with little matrix porosity, but the much deeper cave may have allowed for mixing and attenuation of the chemical signal, which itself may have been minimised as the fire was of low intensity (Coleborn et al., 2019, 2018, 2016a). Dripwater monitoring results highlight that site and sample selection is a key step in speleothem palaeofire research, with sample selection further discussed in Section 5.1. An understanding of cave hydrogeology (through cave monitoring) will facilitate appropriate sample selection.

#### 4.2.5 Impact on organic biomarkers

Organic biomarkers have been extensively used to investigate past fires in ice and sediment cores (Battistel et al., 2018; Brittingham et al., 2019; Thomas et al., 2022; Vachula et al., 2019). In speleothems, organic biomarkers have been applied to investigate climate-terrestrial carbon feedbacks (Wang et al., 2019) and past temperature (Baker et al., 2019; Blyth



et al., 2016; Huguet et al., 2018). The use of organic biomarkers in speleothem research has been limited by the low concentrations of organic matter in speleothems, with analyses generally requiring large sample sizes (up to 20 g), resulting in coarse resolutions (Blyth et al., 2016) and the loss of source signature due to the biodegradation and sorption of organic biomarkers between the source and the speleothem (Blyth et al., 2016; Jex et al., 2014). Additionally, organic biomarker analyses are susceptible to contamination, and require care in sample preparation and laboratory protocols (Blyth et al., 2016; Wynn and Brocks, 2014). However, recent analytical advances have enabled high resolution analysis of polycyclic aromatic carbons in calcite (Argiriadis et al., 2019). This could be significant, as polycyclic aromatic carbons have been extensively used in sediment core fire research (Denis et al., 2012; Vachula et al., 2022). Noting that their low water solubility might limit their concentrations in speleothems, polycyclic aromatic hydrocarbons offer an exciting new application for speleothem palaeoenvironmental research. In speleothems, recent research has shown feasibility, with high-resolution analyses finding detectable concentrations of these hydrocarbons in a stalagmite coinciding with a known fire event over a shallow cave in northwest Australia (Argiriadis et al., 2019).

#### 4.2.6 Impact on mineral magnetism

When sedimentary minerals are heated (e.g. in a hearth or in a wildfire), they undergo magnetic enhancement (Gedye et al., 2000; McClean and Kean, 1993). Mineral magnetism has been used to determine dominant fuel type in Iron Age and Medieval hearths (Peters et al., 2001), to detect Holocene hearths in North America (Urban et al., 2019), and to reconstruct palaeofire from sediment cores (Gedye et al., 2000). Recent advances in microscopy have allowed for speleothems, which typically do not have sufficient concentrations of magnetic minerals for high-resolution palaeomagnetic analyses (Lascu et al., 2016), to be analysed at spatial resolutions of 200  $\mu\text{m}$  or better (Feinberg et al., 2020; Fu et al., 2021; Naoto et al., 2021). Recently, Quantum Diamond Microscopy achieved a mineral magnetism spatial resolution of 4.7  $\mu\text{m}$  on analysis of an annually laminated speleothem from Brazil, finding that changes in magnetism reflected changes in hydroclimate (Fu et al., 2021). These high-resolution techniques have enabled stalagmite hydroclimate reconstructions at temporal resolutions comparable with or exceeding that of conventional methods such as Isotope Ratio Mass Spectrometry (Feinberg et al., 2020; Fu et al., 2021). It has been demonstrated that magnetic enhancement can occur in ash (McClean and Kean, 1993). Following this, there is potential for speleothem palaeomagnetism to record past fire events or past fire regimes, and changes in the magnetic properties of a Tongan speleothem have been tentatively linked to anthropogenic fire use (Naoto et al., 2021).

## 5 Methods and techniques

### 5.1 Speleothem sample selection

Honey to brown coloured calcite generally has higher organic content, with the colour indicating that a speleothem was fed by dripwater that underwent both high soil-water contact and efficient surface-to-stalagmite transport of organics (Pearson et al., 2020; Treble et al., 2017; van Beynen et al., 2001). Inclusion of organic matter is critical for the transport and inclusion of insoluble trace metals which are non-exchangeable in short thin-film residence times, but which may be bound and incorporated in speleothems with organic matter (Hartland et al., 2014, 2011; Pearson et al., 2020). Following this, calcite colour may be used as a simple diagnostic for sample selection. Climates with high seasonality produce stalagmites with annual chemical and

physical laminae (e.g. Orland et al., 2014), which aids in the development of an accurate annual-resolution chronology such as that used by McDonough et al. (2022). McDonough et al. (2022) were able to constrain fire events with a maximum age error of  $\pm 13$  years over a period of  $\sim 250$  years. Faster-growing stalagmites allow for higher temporal resolutions as common analytical approaches require a growth rate of  $> 20 \mu\text{m yr}^{-1}$  to capture annual data, and even higher to capture seasonal data (see Section 5.2 for instrumental spatial resolutions). As stalagmites have been shown to record discrete fire events (McDonough et al., 2022) rather than mean fire behaviour, higher growth rates allow for better confidence around the timing of those events. Globally, stalagmite growth rate has been shown to positively correlate with mean annual temperature (Baker et al., 2021), which suggests that warmer fire-prone regions may be more likely to produce faster growing stalagmites.

High sample porosity, and cracks or poor sample polishing can confound micro-analytical results. For LA-ICP-MS, calcium is used as an internal standard to account for variations in the volume of material ablated but relatively large variations in calcium over porous regions and cracks may introduce an analytical artefact to this correction (Sinclair et al., 1998). For SIMS, these features can interrupt the integrity of sample coating and thus create potential for analytical artefacts. For S- $\mu$ XRF, porous samples, including fluid inclusion-rich samples produce scattering of the fluorescence signal which can significantly affect the clarity of the elemental map. This can be overcome by careful sample selection, petrographical examination of thin sections and comparison with the S- $\mu$ XRF calcite and elastic scattering maps (Borsato et al., 2021).

## 5.2 Lab methods

Here, we provide an overview of methods with applications to the detection of inorganic palaeofire proxies in speleothems, including laser ablation inductively coupled plasma mass spectrometry (LA-ICP-MS) and solution ICP-MS, Synchrotron micro-XFM (S- $\mu$ XRF) and benchtop micro-XFM, U-series dating, carbon dating, and lamina counting, isotope ratio mass spectrometry (IRMS), and secondary ion mass spectrometry (SIMS). As multi-proxy archives, analysis of speleothems for palaeoenvironmental applications generally requires a combination of laboratory methods.

### 5.2.1 Inductively coupled plasma mass spectrometry

Both laser-ablation inductively coupled plasma mass spectrometry (LA-ICP-MS) and solution inductively coupled mass spectrometry (solution ICP-MS) can measure most elements with high analytical precision and low limits of detection. LA-ICP-MS element detection may be hindered by non-carbonate inclusions which cannot be excluded, while solution ICP-MS is mainly limited by elemental interferences (Fairchild et al., 2006; Fairchild and Treble, 2009). LA-ICP-MS has typical detection limits of 0.1-10 ppm (s) and typical spatial resolution of 20-1000  $\mu\text{m}$ , but sometimes as low as 3  $\mu\text{m}$  (Müller and Fietzke, 2016), while solution ICP-MS detection limits can reach ppb levels, with a sample size of 100-5000  $\mu\text{g}$  (100  $\mu\text{g}$  of calcite is  $\sim 0.34 \text{ mm}^3$ ; Fairchild et al., 2006). Advantages of LA-ICP-MS are its rapid and precise measurement, it is minimally destructive, and generally affordable and accessible. Solution ICP-MS is also precise, accurate, affordable and accessible, but sample preparation and analysis are more time consuming and destructive than LA-ICP-MS. A disadvantage of LA-ICP-MS is that false positives can be introduced by cracks, porosity, and imperfections in the sample, as trace

elements are generally presented as a ratio of calcium, and these regions will have lower calcium counts. McDonough et al. (2022) presented five parallel LA-ICP-MS tracks and showed that a decrease in calcium associated with a crack produced a false peak in phosphorous. This can be overcome through careful sample preparation and choice of laser track, and multiple tracks or operating in raster mode may be used to overcome this limitation (Sliwinski and Stoll, 2021; Treble et al., 2005). There is currently no widely-available matrix-matched calcite standard for LA-ICP-MS, and while glass standards are commonly used, they are imperfect (Baldini et al., 2021).

### 5.2.2 Synchrotron micro-XFM and benchtop micro-XFM

Trace element concentrations can vary laterally along growth layers (Treble et al., 2003, 2005), and elemental maps allow lateral heterogeneity to be resolved. While LA-ICP-MS can be used to analyse a wide range of elements with very low detection limits (Treble et al., 2005; Woodhead et al., 2007), resolution is limited to  $\sim 20 \mu\text{m}$  (Borsato et al., 2021; Sliwinski and Stoll, 2021). X-ray fluorescence (XRF) or X-ray fluorescence microscopy or mapping (XFM) allows for the quantification of elements through the bombardment of a sample (e.g. speleothem calcite) with high energy primary X-rays (Ramsey et al., 1995). This bombardment removes inner shell electrons, and as outer orbit shell electrons fall to lower energy orbitals, they fluoresce characteristic secondary X-rays which may be measured to quantify elemental concentrations (Ramsey et al., 1995; Scroxton et al., 2018). Both S- $\mu$ XRF and benchtop micro-XFM have been used to analyse speleothems.

S- $\mu$ XRF can produce elemental maps with resolutions as high as  $1 \mu\text{m}$  per pixel (Borsato et al., 2021). As mean annual growth rate for laminated speleothems is  $\sim 160 \mu\text{m yr}^{-1}$  (Baker et al., 2021), the very high resolution provided by S- $\mu$ XRF allows for sub-seasonal data to be collected (Baldini et al., 2021). As well as changes in chemical concentration, S- $\mu$ XRF can visualise changes in porosity and large-scale variation in speleothem fabric (Borsato et al., 2021, 2007; Frisia et al., 2005; McDonough et al., 2022). Accompanying X-Ray Absorption Near Edge structure can be used to determine chemical speciation (Baldini et al., 2021; Frisia et al., 2008). S- $\mu$ XRF limits of detection depend on the excitation energy, dwell time, porosity, pixel size, and detector type, and tend to be higher than for LA-ICP-MS (approximately 10-100 ppm for S- $\mu$ XRF). While S- $\mu$ XRF is non-destructive it does require that samples be sectioned to fit the mount, polished or double-polished, and sample preparation can impact results (Borsato et al., 2021). In calcite, high excitation of Ca, and escape and sum peaks of the same, can interfere with nearby elements (Borsato et al., 2021). A significant disadvantage of S- $\mu$ XRF is the expense, although merit-based free access can be achieved for many of the world's research synchrotrons. Borsato et al. (2021) and Baldini et al. (2021) present comprehensive guides to the application of S- $\mu$ XRF to speleothems.

Micro-XFM is a more commonly available alternative technique but with a lower-energy compared with S- $\mu$ XRF that produces a compromise on resolution and detection limits. Some non-vacuum micro-XFM have the advantage of being able to analyse full sample lengths. Non-vacuum 'benchtop' and core-scanner micro-XFM has been used to measure heavier elements such as strontium, iron, silicon, copper, potassium, nickel and barium (Buckles and Rowe, 2016; Guo et al., 2021; Scroxton et al., 2018; Tan et al., 2015; Wu et al., 2012), but lighter elements (e.g. magnesium) are generally confounded by the attenuation of secondary X-rays in the air-gap (Scroxton et al., 2018). Vacuum or near-vacuum micro-XFM may enable the analysis of lighter

elements such as sulphur or magnesium. However, recently sulphur was successfully measured using benchtop non-vacuum micro-XFM, with artefacts due to the diffraction of the incident beam overcome by the use of multi point statistics (Wang et al., 2022). The ability to measure strontium by micro-XFM is a key advantage, as it allows for the rapid and economic development of Sr-based chronologies in annually laminated samples.

### 5.2.3 Chronology building

Uranium-series techniques (e.g. U-Th disequilibrium, U-Pb, (U-Th)/He) are used to absolutely date speleothems at scales from the modern to millions of years old (Fairchild and Baker, 2012; Makhubela and Kramers, 2022; Richards et al., 1998). They are based on the radiogenic decay of uranium isotopes ( $^{234}\text{U}$ ,  $^{235}\text{U}$ , and  $^{238}\text{U}$ ), whose half-lives are well-constrained (Cheng et al., 2000; Jaffey et al., 1971; Rasbury and Cole, 2009), to various daughter isotopes. U-Th disequilibrium dating generally has high precision ( $\sim 1\%$ ) but may be complicated by the inclusion of 'detrital' thorium (Fairchild and Baker, 2012; Zhao et al., 2009). Detrital thorium is transported with organic matter, colloids, and sediments and may result in overestimation of the U-Th age without correction (Fairchild and Baker, 2012). U-Th dating is challenging in young carbonates where the daughter  $^{230}\text{Th}$  is very low, and may be confounded by the presence of non-radiogenic  $^{230}\text{Th}$  (Zhao et al., 2009). Non-radiogenic  $^{230}\text{Th}$  may form a greater proportion of total  $^{230}\text{Th}$  in young carbonates, and so have a greater impact in young carbonates than in old carbonates (Zhao et al., 2009). Precision of the U-Th geochronometer declines after  $\sim 400$  ka (Fairchild and Baker, 2012). U-Pb dating has slightly lower precision than U-Th dating (1-5%), but can be applied to much older carbonates ( $>400$  Ma) (Fairchild and Baker, 2012). As with the U-Th geochronometer, U-Pb dating may be complicated by detrital lead as well as variable initial Pb (Fairchild and Baker, 2012; Rasbury and Cole, 2009). The problem of common Pb may be overcome by screening for detrital Th, as they are likely to have the same source (Fairchild and Baker, 2012; Woodhead et al., 2006). Recently, (U-Th)/He dating has been applied to South African speleothems (Makhubela and Kramers, 2022). (U-Th)/He is an alternative to U-Pb for samples older than 500 ka, and has some advantages in that more He atoms are produced per decay than Pb, and He is not expected to be included in speleothems other than by radiogenic decay (Makhubela and Kramers, 2022). As such, (U-Th)/He dating may be a suitable method for dirty samples and samples low in uranium (Makhubela and Kramers, 2022), although apatite and zircon He ages may be reset by wildfire (Mitchell and Reiners, 2003), which could complicate (U-Th)/He dating of speleothems.

Carbon dating of speleothems is complicated by the processes which transport atmospheric  $^{14}\text{C}$  to calcite. Bedrock, soil, and occasionally cave atmosphere all contribute carbon to speleothems. The potentially large and variable proportion of bedrock-derived carbon, which is termed 'dead carbon' as all  $^{14}\text{C}$  has generally decayed (except in very young parent rocks) must be accounted for to accurately use  $^{14}\text{C}$  as a geochronometer in speleothems (Fairchild and Baker, 2012; Hua et al., 2012). However, in modern samples, the 'bomb-pulse' may be used as a chronological anchor to constrain 20th Century speleothem growth (Genty and Massault, 1999; Markowska et al., 2019). Hua et al., (2012) demonstrated that when the dead carbon fraction can be determined and corrected for, reliable  $^{14}\text{C}$ -derived chronologies can be achieved, while Lechleitner et al. (2016) have developed an algorithm to date speleothems independent of the dead carbon fraction (although it does require that the dead carbon fraction has no long-term trend. Nonetheless, radiocarbon dating is probably best-reserved for young speleothems, where U-series techniques are not applicable.

Speleothems may form both physical and chemical annual laminae, and stalagmites which form annual laminae are most common where precipitation is highly seasonal (Baker et al., 2021). In a global synthesis of annually-laminated stalagmites, Baker et al. (2021) observed centennial-scale stability in stalagmite extension rates, with climate forcing of growth rate variations observed only where the multi-year climate signal was large enough to dominate the calcite extension rate. This suggests that annual lamination is robust enough to persist through climate fluctuations, and therefore be a reliable addition to chronology-building (Baker et al., 2021). Annual laminae for improving speleothem chronologies are especially useful where radiometric dating uncertainties are high due to (for example) low environmental uranium/high initial  $^{230}\text{Th}$ , as seen in the Tropical Pacific, or insufficient ingrowth of  $^{230}\text{Th}$ , as seen in modern speleothems. Smith et al. (2009) used chemical variations obtained by ion microprobe to date non-laminated Alpine speleothems. More recently, Faraji et al. (2021) used S- $\mu$ XRF mapping of strontium concentrations and optical imaging of stalagmite laminae to generate an annual chronology with a maximum of  $\pm 15$  years of uncertainty over the 336-year record. In modern speleothems from southwest Australia (a region with a Mediterranean climate with strong seasonality and seasonal controls on prior calcite precipitation), annual fluctuations in trace element concentrations have been used to construct chronologies for modern stalagmites with low uncertainties (McDonough et al., 2022; Nagra et al., 2017).

#### 5.2.4 Isotope ratio mass spectrometry

Stable carbon and oxygen isotopes may be measured with isotope ratio mass spectrometry, typically by milling discrete samples, although laser-ablation techniques exist (Spötl and Matthey, 2006). While laser ablation is much more time-efficient, the use of the laser adds additional fractionation to not just the ablated sample but also to the ablation pit and the thermal halo, which can be 2–4 times the size of the laser spot (Fairchild et al., 2006; Spötl and Matthey, 2006). Milled IRMS has better external precision than LA-IRMS, and can achieve better spatial resolution (as low as 0.05 mm) (Fairchild et al., 2006), although disadvantages are that milled IRMS is more destructive and resolution can be variable depending on the density of the material (with sample weights of 50–120  $\mu\text{g}$  typically required).

#### 5.2.5 Secondary ionisation mass spectrometry

Secondary Ion Mass Spectrometry (SIMS) can measure both trace elements and stable isotope ratios in carbonates. SIMS is minimally destructive, requiring only a very small amount ( $< 1$  ng) of material. However, sample preparation requires sectioning, polishing and mounting, leading to some loss of material. SIMS has excellent lateral resolution for both trace elements (1–2  $\mu\text{m}$  spot size) and stable isotope ratios ( $\sim 10$   $\mu\text{m}$ ), meaning it is capable of producing seasonal-resolution data (Baldini et al., 2021; Orland et al., 2019). However, sample size is restricted to  $< 15$  mm, which along with the comparatively long analysis duration (e.g., 3–4 min per  $\delta^{18}\text{O}$  spot analysis, complicates the construction of long seasonal records. A clear advantage over LA-ICP-MS is that SIMS can overcome polyatomic interferences from  $^{48}\text{Ca}$  and  $^{16}\text{O}$  and measure sulphur (Wynn et al., 2010), which is valuable in palaeofire research as sulphur has been shown to be a key indicator of past fire (McDonough et al. 2022).

### 5.3 Statistical approaches

Statistical methods can be used to identify the timing of fire events. McDonough et al. (2022) used timeseries Principal Component Analyses (PCA) and k-means clustering of variables to

identify key processes affecting stalagmite geochemistry. Both PCA and clustering approaches are widely used in speleothem science to analyse multivariate datasets (e.g. (Markowska et al., 2015; Nagra et al., 2017; Orland et al., 2014). McDonough et al. (2022) identified dry and wet periods, the contributions of bedrock- vs aerosol-derived parameters, and short-term increases in phosphorus and trace metals including zinc, lead, copper and aluminium which aligned with the timing of known fire events occurring over the cave. They concluded that increases in phosphorous and trace metals were the likely result of soluble and colloidal ash-derived elements entering the dripwater and being incorporated into the speleothem. Identification of changes in dry and wet conditions allowed for an observed change in hydrology after a particularly intense fire event resulted in a decrease in water-rock interaction and dilution of bedrock and aerosol sourced components (McDonough et al., 2022). McDonough et al. (2022) found that peaks in their ‘fire’ principal component were not always driven by peaks in the same elements, and that no single chemical tracer could identify each fire event, highlighting that a multivariate statistical approach was required. McDonough et al. (2022) also used changepoint analysis to identify which parameters were most affected by these longer-term changes in hydrology, although they found that changepoints were not suitable for identifying short term changes in trace metals and phosphorus. Hope et al. (2010) previously used changepoint analysis to identify dry periods in rainfall timeseries data, while Tibby et al. (2018) used the same approach to analyse proxy rainfall data. Their results suggest this technique could be useful for detecting changes in climate and hydrology leading up to, or following, fire events, but less useful for identifying individual fire events.

## 6 Southwest Australian case studies

Here, we present four case studies which illustrate [1] that ash geochemistry is related to fire severity, [2] how sulphur cycling is impacted by fire events [3] how a catastrophic palaeofire in southwest Australia was related to changed land management and climate, and [4] that fires may be recorded in deep cave stalagmites, if hydrological processes allow the transport of the fire signal. These case studies are drawn from published and unpublished research, and analytical methods for each case study except the third (published in full in McDonough et al., 2022) are presented in the supplemental material.

### 6.1 Geochemistry of bushfire ash leachates

Ash from fires can alter soil and cave dripwater chemistry. This ash can form directly on soils above a cave after a fire, or be transported into the region via surface runoff and winds. Cave dripwater may be impacted through leaching of the ash and transportation of elements as either soluble ions or colloids (both bound to organic matter and as particulates) (Hartland et al., 2012). The composition of wildfire ash derived from the burning of biomass is a function of the plant species burned and the extent of their bioaccumulation of elements, burn temperature and combustion completeness (Bodí et al., 2014). Ash colour is related to the combustion completeness (Roy et al., 2010; Stronach and McNaughton, 1989). Black char is the primary by-product of biomass pyrolysis and occurs at low temperatures ( $\leq 350^\circ\text{C}$ ; Bodí et al., 2014), while white ash occurs when vegetation is at or near complete combustion ( $500\text{--}1400^\circ\text{C}$ ; Bodí et al., 2014). Elements with high volatilisation temperatures, such as potassium, zinc, cadmium, copper, sodium, magnesium, calcium, and manganese (all  $>700^\circ\text{C}$ ) increase in relative proportion to other elements at higher burn temperatures, due to the removal of other elements such as nitrogen and sulphur at lower temperatures ( $<600^\circ\text{C}$ ; Figure 4).

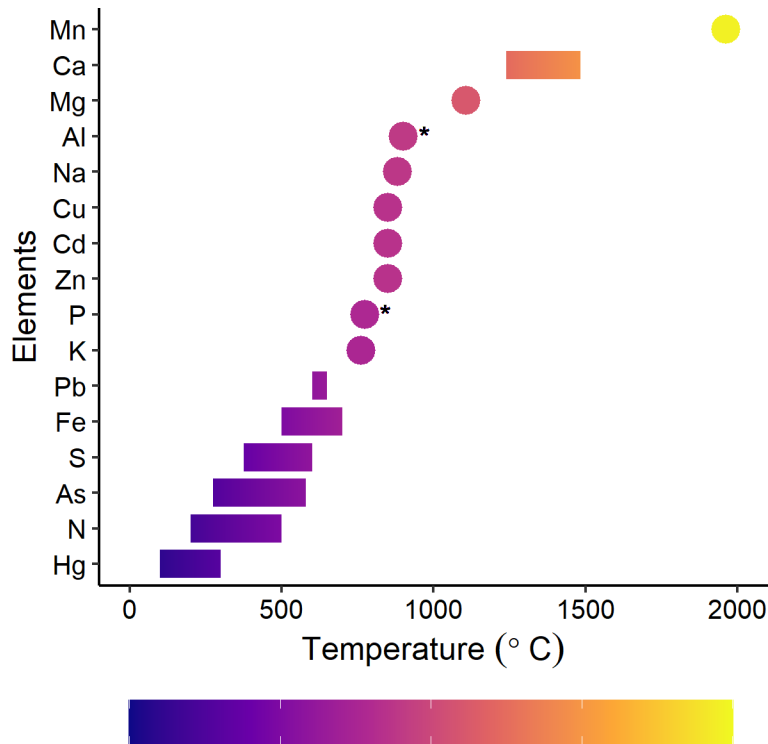


**Figure 4** Volatilisation temperatures for select elements. Bars show the range of temperatures reported, while circles show singular values. The asterisk (\*) indicates that this is a minimum volatilisation temperature, with the actual temperature likely to be higher. Colour indicates temperature in °C, the colour bar is to the same scale as the x-axis. Mn, Ca, Mg, Na, K, S, N and Hg volatilisation temperatures reported in Bodí et al. (2014) and references therein. Zn volatilisation temperature from Clifford et al. (1993), Pb, As, Cd and Cu volatilisation temperatures from Tuhý et al. (2021), Fe, and Al volatilisation temperatures from Balfour and Woods (2013). P volatilisation temperature as reported in Bodí et al. (2014) and Balfour and Woods (2013). Note that different terminologies and experimental designs were used. Adapted from Bodí et al. (2014).

While few studies have investigated the concentrations of heavy metals in ash, or how these vary with plant species composition and burn temperature, Pereira and Úbeda (2010) reported that concentrations of aluminium are higher than other metals leached from ash after the burning of oak and pine trees. They also identified high variability in iron and zinc concentrations, with lower concentrations associated with upslope locations which was suggested to be the result of greater burn temperatures. Since trace metals are usually present in very low concentrations in uncontaminated soils, increases in concentrations due to the leaching of ash could be a useful indicator of past fire events in speleothems. In addition, nutrients such as phosphorous and sulphur can be present in high concentrations in plant ash (Etiegni et al., 1991; Sander and Andrén, 1997) and may also be a useful proxy for past fire events. The addition of plant ash to soils has been observed to result in the leaching of 3—10 times more phosphorus from soils compared to soils that do not contain ash (Escudey et al., 2010). McDonough et al., (2022) identified that trace metals and nutrients such as phosphorous from ash were useful fire proxies in a speleothem, however the combination of phosphorous and trace metals that

increased during known fire events above the cave was found to be inconsistent. The authors hypothesised this to be the result of differences in fire intensities.

Ash leachate analyses on white and black ash collected after a wildfire in Yanchep National Park, Western Australia, in December 2019 are presented below (Figure 5). Boxplots show clear and statistically significant differences in concentrations of phosphorous, sulphur, sulphate, zinc, aluminium, iron, copper, and magnesium. Strontium concentrations are not significantly different, although white ash results are more variable. This is a positive outcome as it suggests that strontium in speleothems is unlikely to be impacted by fire events, and so strontium-based chronologies are robust to fire impacts, at least for this karst region where strontium has been shown to be bedrock derived (Treble et al., 2016). Generally, ash leachate results are consistent with volatilisation temperatures from the literature (Figure 4). That is, elements with very high volatilisation temperatures have higher relative abundances in white ash (e.g. magnesium and copper), while elements with lower volatilisation temperatures have higher relative abundances in black ash (e.g. phosphorous and zinc). Our data also show this same pattern in Al and Fe, but our literature review did not locate soil or vegetation volatilisation temps for those elements. Sulphur and sulphate are the exception, having high concentrations in white ash, despite S volatilising at a relatively low temperature. Similar results have been reported for sulphate in an analysis of global ash leachates, although analysing ash chemistry as a function of fire intensity was not the primary aim of that research (Harper et al., 2019). Differences in ash-derived metals measured in speleothem archives are hypothesised to differentiate between the intensity of palaeofires, and is an area of future research.



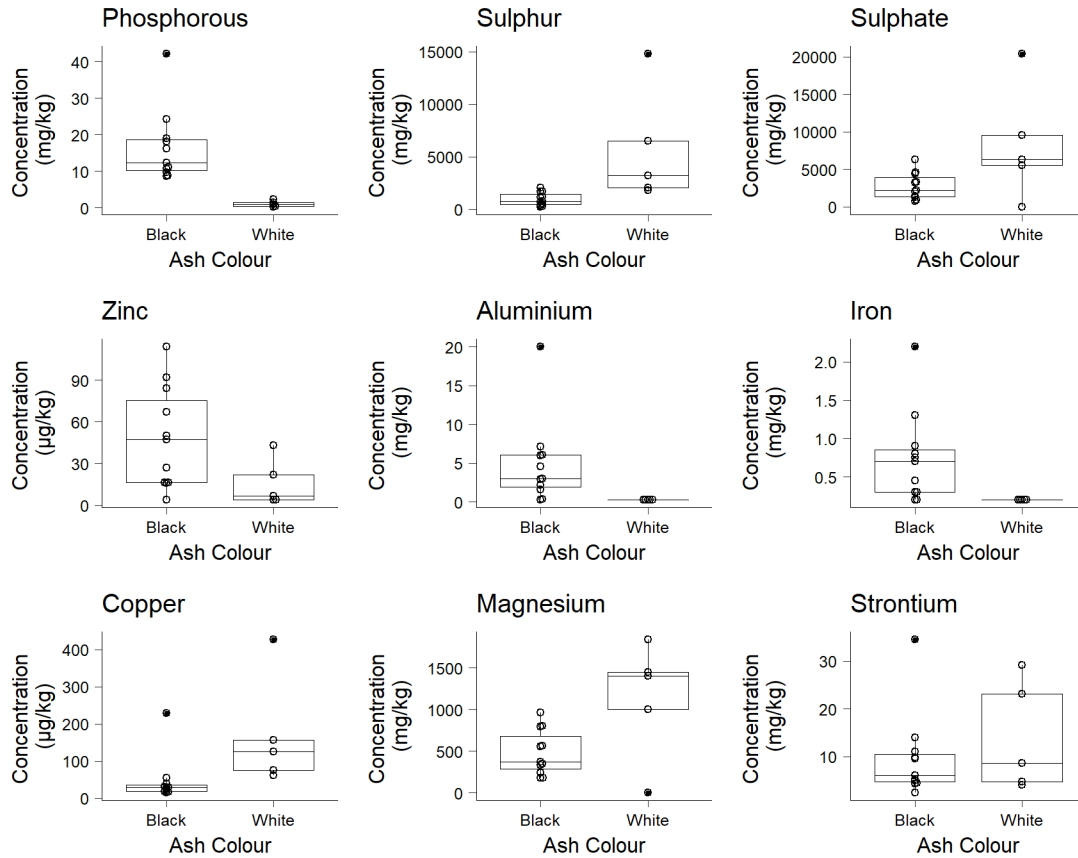


**Figure 5** Boxplots of ash leachate concentrations by ash colour. Individual data points are overlaid and slightly offset from one another to reduce overlap.

## 6.2 Sulphur as a proxy for post-fire recovery

Treble et al. (2016) observed a declining trend in dripwater sulphate over the duration of a dataset between 2005—2015 CE. This was demonstrated by mass balance to represent a net loss (sink) of sulphate over the studied interval in the Golgotha Cave system, southwest Australia (Treble et al., 2016). Mass balance also identified that the source of sulphate in dripwaters at this site is  $\geq 62\%$  marine aerosol, consistent with the coastal location (Treble et al., 2016). Analysis of dual sulphate isotopes ( $\delta^{34}\text{S-SO}_4$   $\delta^{18}\text{O-SO}_4$ ) in the rainfall at this site confirmed the main source of sulphate to be of marine origin. The dual sulphate isotopes in the dripwaters ( $n=4$ ) suggested that the sulphate sink identified through element mass balance, was due to sulphur sequestration into biomass, and attributed to the post-fire recovery of the forest understorey following fires that impacted the site in 1992 and 2006 CE (Treble et al.; 2016). The post-fire recovery interpretation was also supported by rising dripwater chlorine trends interpreted to represent increasing transpiration as the shrubby understorey recovered (Treble et al.; 2016).

SIMS measurements of stalagmite sulphur and chlorine concentrations from a stalagmite (GL-S4) sampled from one of the monitored dripwater locations in Golgotha Cave are shown in Figure 6 together with dripwater chlorine and sulphate (Coleborn, 2020). The stalagmite data (1926—2005 CE) enabled a longer-term examination of the trends detected in the dripwater. It

revealed that the observed decline in dripwater sulphate was a continuation of a trend which began at least five decades earlier, commensurate with the largest known wildfire to have impacted the forest above and surrounding the cave area which occurred in 1961, and not only after less severe wildfires in 1992 or 2006, as previously thought (Treble et al., 2016). The stalagmite chlorine concentration trend also switched at around this time, providing strong evidence that these observed trends in sulphur and chlorine are due to the 1961 fire (Figure 6). Figure 6 also shows the dripwater chemistry data extended to 2021. Recent reversal of the downward trend in dripwater sulphate may be attributed to reduced sulphur uptake by overlying vegetation, which has now reached maturity, or the domination of the transpiration signal (indicated by the increase in the chlorine rise around the same time) in a region experiencing prolonged drying.

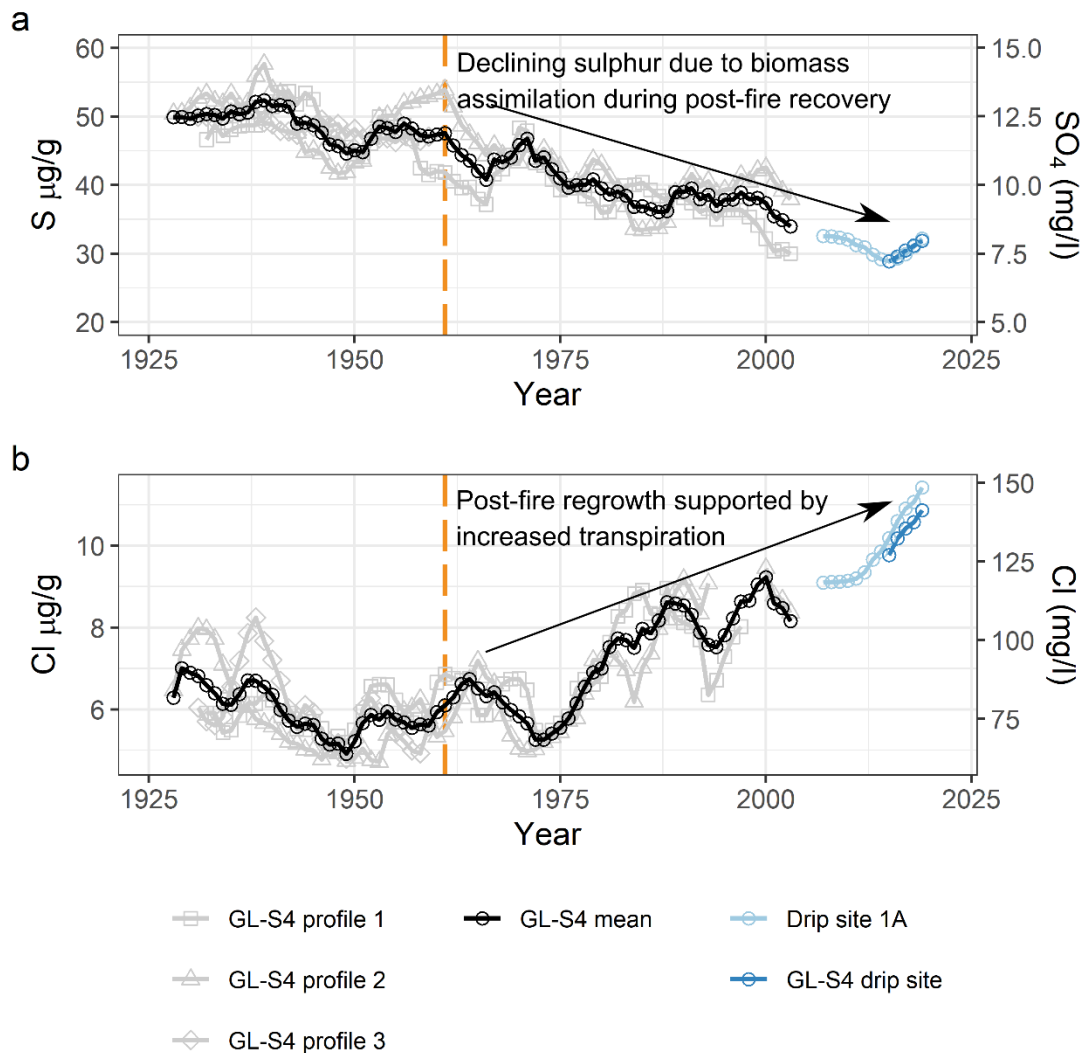


**Figure 6** Time series of stalagmite and dripwater S and  $\text{SO}_4$  (a) and Cl (b) concentrations from Golgotha Cave, southwest Australia. Data are aggregated annually and presented as a running 5-year mean. Drip site 1A is close to the sampling site of GL-S4 (~1 m). The orange dashed line indicates the 1961 fire, while black arrows indicate the trend in sulphur and sulphate (a) and

chlorine (b). The right-hand axis is scaled to visualise the continuation of the GL-S4 sulphur and chlorine trends.

Subsequent and more comprehensive analyses of dual sulphate isotopes of dripwater, bedrock, and rainfall is summarised in Table 2, together with  $\delta^{34}\text{S}$  analyses of vegetation and soil. The expanded  $\delta^{18}\text{O}\text{-SO}_4$  and  $\delta^{34}\text{S}\text{-SO}_4$  isotopic data for rainfall confirmed that the sulphate was from a marine source (Table 2). Sulphate reduction was ruled out as a potential cause of the sulphate sink as this would result in higher dripwater  $\delta^{18}\text{O}\text{-SO}_4$  values compared with rainfall, whereas the opposite was observed (Table 2). Mean dripwater  $\delta^{18}\text{O}\text{-SO}_4$  values were lower than rainfall by 4.1‰, strongly supporting biogeochemical cycling of the input rainfall signal before reaching the cave under oxidising conditions. Mean  $\delta^{34}\text{S}\text{-SO}_4$  of dripwaters were ~1‰ higher than rainfall (Table 2). This is theoretically consistent with biomass assimilation, which results in ~1—2‰ fractionation due to preferential assimilation of  $^{32}\text{S}$  (Marty et al., 2011; Wynn et al., 2013). Vegetation appeared to support similar  $\delta^{34}\text{S}$  values to those observed in the cave drip waters (Table 2; Coleborn, 2020). No observable counterpart fractionation to lighter isotopic values in the vegetation due to assimilation is likely due to a pool size effect, with vegetation representing the biggest sink of sulphur in the system. Bedrock was found to contribute <5% of  $\text{SO}_4$  to dripwaters.

**Table 2** Dual  $\text{SO}_4$  isotope values for rainfall, cave dripwater, and bedrock from Golgotha Cave, southwest Australia.  $\delta^{34}\text{S}$  results for vegetation and soil samples from the Golgotha Cave region. Mean values presented with minimum and maximum values reported in brackets, n shows the number of replicates. Vienna Standard Mean Ocean Water (VSMOW) was the  $\delta^{18}\text{O}$  standard, and Vienna-Canyon Diablo Troilite (VCDT) was the  $\delta^{34}\text{S}$  standard. Data from (Coleborn, 2020).

|                | $\delta^{18}\text{O}\text{-SO}_4$ (‰ VSMOW) |                     | $\delta^{34}\text{S}\text{-SO}_4$ (‰ VCDT) |                          | $\delta^{34}\text{S}$ (‰ VCDT) |                        |
|----------------|---|---------------------|--|--------------------------|--------------------------------|------------------------|
|                | n   |                     | n  |                          | n                              |                        |
| Rainfall       | 6   | +8.1 (+6.9 to +9.7) | 7  | +18.8 (+17.8 to +19.8)   | 0                              | -                      |
| Cave dripwater |   |                     |  |                          | 0                              | -                      |
| 1A             | 8   | +4.0 (+1.4 to +6.1) | 9  | +20.1 (+18.5 to +21.7) 8 | 0                              | -                      |
| 1IV            | 0   | -                   | 1  | 19.6                     | 0                              | -                      |
| Bedrock        | 1   | +7.8                | 1  | +18.7                    | 0                              |                        |
| Vegetation     | 0   | -                   | 0  | -                        | 31                             | +20.5 (+17.9 to +22.1) |
| Soil           | 0   | -                   | 0  | -                        | 20                             | +19.1 (+17.8 to +20.3) |

Results presented here suggest that speleothem sulphur may be useful as a proxy for fire due to the observed multi-decadal duration of reduced sulphur concentrations, attributed to increased biomass assimilation as a forest recovers after fire. This approach would likely be limited to sites where the supply of sulphur becomes source limited for a prolonged period after fire and where sulphur supply is not complicated by multiple sources. Dual sulphate isotopes

may assist in characterising the latter, and theoretically could be applied to speleothems (as could  $\delta^{34}\text{S}$  measured in situ) to detect disruptions in biomass cycling due to fire. It is also recognised that sulphur incorporation into speleothems may be dominated by pH control (Wynn et al., 2018, 2014). For example, sulphur was examined in stalagmite YD-S2, also from southwest Australia (McDonough et al, 2022). In that study, only a short-term depletion in sulphur was observed, directly coinciding with an inferred intense fire in 1897 ( $\pm 5$  years). This was attributed to either volatilisation of sulphur and/or an increase in dripwater pH caused by calcination of the limestone above the cave (McDonough et al, 2022). That speleothem-based paleo-fire record is further examined in the third case study (Section 6.3). Further development work on sulphur as a fire proxy in speleothems is required.

### 6.3 Catastrophic palaeofire and links to climate and land management

McDonough et al., (2022) used LA-ICP-MS, S- $\mu$ XRF, and stable isotopes ( $\delta^{18}\text{O}$  and  $\delta^{13}\text{C}$ ) to compare the speleothem proxy response to recent known fires and to apply this to reconstruct past fire frequency in a stalagmite from a shallow ( $< 6$  m depth) cave in Yanchep, Western Australia. A particularly intense paleo-fire was identified to have occurred in 1897  $\pm 5$  CE identified by changes in fabric and both short and long-term changes in the isotopic and elemental composition. They identified a short-term peak in  $\delta^{18}\text{O}$  just after the 1897 CE fire, understood to have resulted from evaporation of soil and karst stores from the fire. This evaporation also resulted in short-term peaks in other bedrock derived parameters including strontium and magnesium (Figure 7). Of note was a large short-lived peak in phosphorous (Figure 7) which exceeded 6 times the concentrations of phosphorous anywhere else in the 245-year record, and a smaller spike in zinc. These were taken to have been derived from ash which was leached into dripwater and incorporated into the stalagmite post-fire. An increase in porosity of the sample for approximately 5 years after the fire was interpreted to have occurred due to the occlusion of growth sites by impurities from ash. The authors also identified an increase in organic matter content post-fire, and a decline in bedrock-derived parameters, suggesting an increase in fracturing and porosity caused by intense heating and cooling of the limestone. This appears to have allowed for reduced physical filtering of OM, and reduced water-rock interaction resulting in higher concentrations of OM and lower concentrations of bedrock-derived elements in the decades following the fire event.

The 1897 $\pm 5$  years fire came at a critical point in Australia's colonial history. Prior to establishment of the Swan River Colony in 1829, the Noongar people had practiced land management through the use of frequent low-intensity burns (Hallam, 2014). By the late 1800s, they had been prevented from practicing cultural burning for 30-60 years (Abbott, 2002; Hallam, 2014). McDonough et al. (2022) suggested that a subsequent build-up of fuel, combined with antecedent dry conditions in the late 19<sup>th</sup> Century may have resulted in this large fire in 1897 CE. This adds to a growing body of work that has linked the cessation of Indigenous land practices to broad-scale landscape change and subsequent higher risk of catastrophic wildfires (Fletcher et al., 2021b; Mariani et al., 2022)

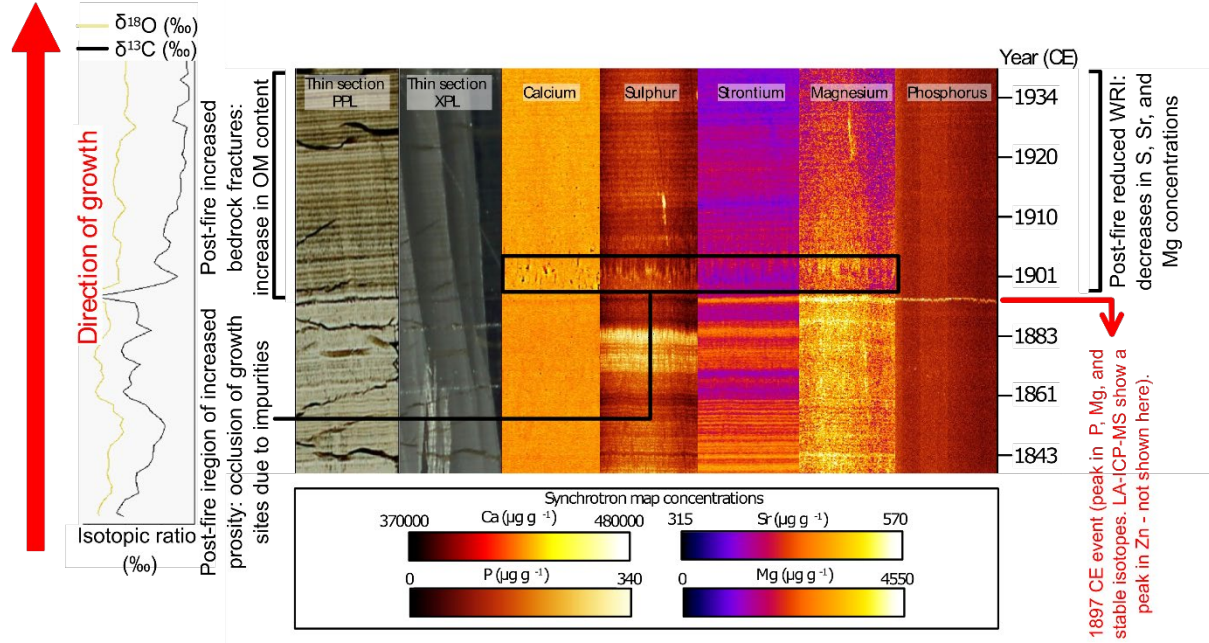


**Figure 7** Plane polar light (PPL) and cross polar light (XPL) thin section scans and S- $\mu$ XRF maps from a sub-section of stalagmite YDS2. An inferred fire event in 1897 CE is identified in McDonough et al. (2022), coinciding with a short-lived peak in phosphorus, strontium and magnesium. A post-fire increase in porosity is evident in the Ca, S and Sr maps, likely due to occlusion of growth sites by impurities. Post-fire impacts such as increases in organic matter (OM) incorporation and decreases in bedrock-derived parameters such as Mg, Sr and S due to increased or widening of fractures after heating and cooling of the bedrock, and subsequent reduced water-rock interaction (WRI), are visible through the darkening of the S, Sr and Mg maps after 1897 CE. Figure adapted from McDonough et al. (2022).

#### 6.4 Fires recorded in deep caves

Dripwater monitoring (Figure 3) and McDonough et al. (2022) showed that infiltration to shallow caves could transport a fire signal which could then be recorded in speleothem calcite. Evidence from dripwater monitoring appeared to indicate that deep caves would not record fires (see Section 4.2). Coleborn et al. (2018; 2019) found no significant change in post-fire dripwater chemistry in a 40 m deep cave in southeast Australia. However, recent (unpublished) data from a deep (~40 m) cave from southwest Australia has demonstrated that deep cave stalagmites (stalagmite CRY-S1) may be able to record fires. Following methods outlined in McDonough et al. (2022) S- $\mu$ XRF analyses of a speleothem collected from Crystal Cave in southwest Australia showed increases in zinc and iron (Figure 8), and distortion of the speleothem fabric following large forest fires over the site in 1961, the same fire that impacted Golgotha Cave in our second case study. Zinc and iron concentrations at the 1961 event were >600 ppm and >1000 ppm, respectively. Outside of the 1961 fire layer, zinc concentrations were ~50 ppm and iron

concentrations were ~200 ppm. The 1961 fire was a large and intense fire which occurred during the catastrophic 1960-61 Western Australian fire season, and which burned >40 000 ha. The fire season was preceded by an anomalously wet winter. -The calcium and strontium maps show the fabric is impacted around the 1961 event (Figure 8), with increased porosity and new crystal growth impacted by renucleation and competitive growth after foreign particle poisoning of the calcite. The high strontium is likely an artefact from scattering of the differently orientated crystals during this competitive growth phase. Other known fires burned over Crystal Cave in 1972, 1975, and 1991, although only the 1972 prescribed fire event is evident in the S- $\mu$ XRF trace element maps, with spikes in iron observed (Figure 8). The 1972 fire was also preceded by an anomalously wet winter, although as a prescribed burn the climatic precursors may have been less relevant. The CRY-S1 chronology is well-constrained and based on annual S- $\mu$ XRF strontium bands.

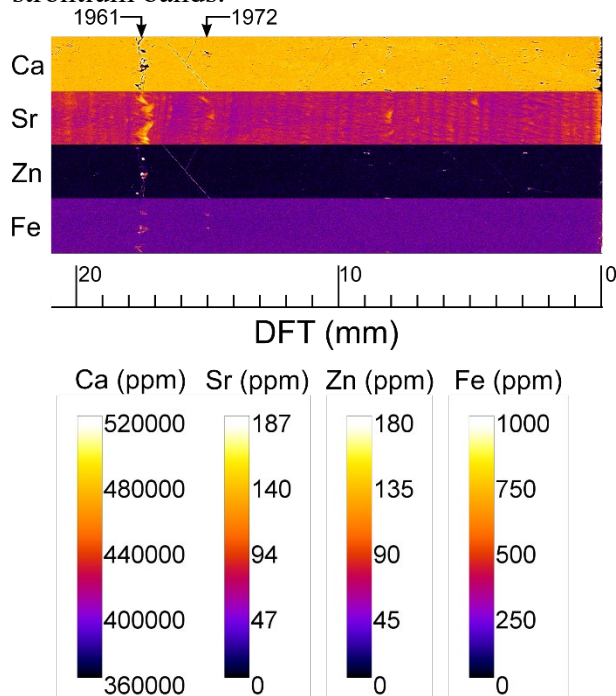


**Figure 8** S- $\mu$ XRF map of modern calcite from Crystal Cave (CRY-S1), in the Margaret River Region of southwest Australia.

The Tamala Limestone of southwest Western Australia has high primary porosity but fracture flow is also an important contribution to dripwaters (Treble et al., 2022). Focussing of flow along fractures may explain how a stalagmite from such a deep cave could have recorded a fire event. This suggests that hydrogeology is just as important as cave depth for the transport and incorporation of a fire proxy signal. That the 1961 wildfire event is so clear in the S- $\mu$ XRF while later prescribed burns are either missing (1975, 1991) or less clear (1972) suggests that this deep cave may act as a fire severity filter, with the CRY-S1 stalagmite recording only severe bushfires. Additionally, since the fire signal is predominantly due to the dissolution and transport of ash-derived elements (see Section 4.2) transport of that signal requires soil hydrological connectivity. This reinforces the necessity of choosing speleothem samples that have efficient surface-cave transport with minimal mixing to minimise the attenuation of the fire proxy signal.



Detecting a fire signal at depth in a highly porous young limestone shows promise for fire signal detection in older limestones where fracture flow is more likely.

Unlike the previous case study and dripwater observations, where an anomaly in  $\delta^{18}\text{O}$  was associated with fires, CRY-S1 shows no change in  $\delta^{18}\text{O}$  after the large bushfire in 1961, or after subsequent prescribed burns in 1972, 1975, or 1991 (Figure 9). This absence of a  $\delta^{18}\text{O}$  response may be associated with local karst processes, cave depth, past land use, and long-term climate and precipitation patterns. This is an important find for the community as it suggests that  $\delta^{18}\text{O}$  hydroclimate records from deep caves are less likely to be impacted by wildfires.

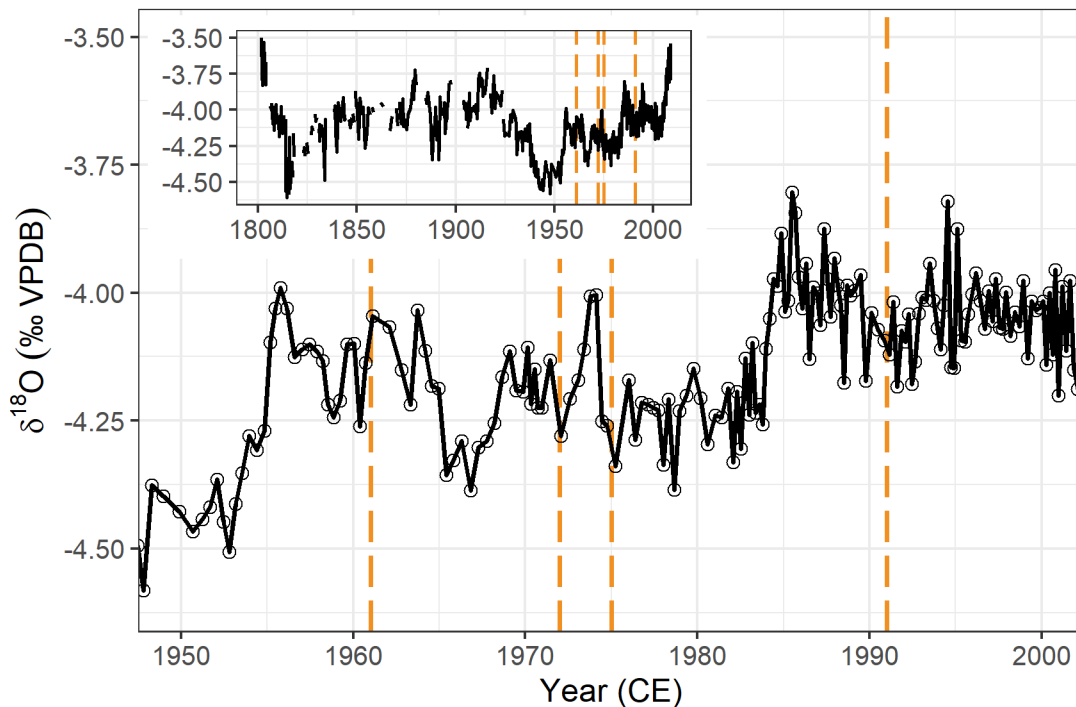


**Figure 9**  $\delta^{18}\text{O}$  record for speleothem CRY-S1, with bushfires in 1691, 1972, 1975, and 1991 indicated by orange dashed lines. The inset shows the full  $\delta^{18}\text{O}$  record for this sample.

## 7 Summary and future research directions

Speleothems offer an exciting new field of research for investigating past fire regimes. Modern analytical and computational advances have allowed for the high-resolution analyses of speleothem trace elements, stable isotopes, and fabric. Robust palaeofire reconstructions are necessary to better understand future wildfire regimes in relation to climate change, to better appreciate ecosystem resilience and the interplay between climate and land management, and to improve data-model comparisons. Below, we discuss where speleothems fit in the palaeofire archive landscape, highlight that speleothem palaeofire research is only possible because of analytical and computational advances, discuss how new knowledge about fire proxies may impact  $\delta^{18}\text{O}$ -derived climate reconstructions, detail how the SISAL V2 database may be used to identify suitable samples for palaeofire research, and discuss future research questions.

While many proxy archives already exist to investigate past fire, speleothems offer a complimentary new archive. The benefits of speleothems are clear: they are absolutely dateable,

recoverable from most continents, and include a range of proxies. Collectively, this makes them ideal candidates for high resolution, precisely dated, palaeofire reconstructions. Additionally, ash is the source of the majority of inorganic fire proxies in speleothems. Ash is a fire end-member that is typically not preserved in existing fire proxy archives and so speleothems offer a unique opportunity to preserve chemical signals from this fire end-member, and speleothem-derived fire reconstructions will compliment sedimentary fire proxy reconstructions, which are typically based on charcoal preservation.

Analytical and computational advances have been critical for the development of speleothems as fire proxy archives. McDonough et al. (2022) clearly demonstrated that S- $\mu$ XRF is a key analytical tool for the detection and precise dating of fire events in speleothems. New results presented here for stalagmite CRY-S1 which demonstrate that speleothems from a deep cave may record past fires also highlight the necessity of S- $\mu$ XRF analyses by showing that some key trace metals (e.g., Fe) are inconsistently deposited along the growth layer. 2-D Elemental mapping identified these inconsistent peaks in trace metals which may have been missed by LA-ICP-MS line scans (see Section 6.4). Computational advances and the generosity of open-source developers mean that complicated multivariate statistical analyses, such as principal component analysis, can now be performed quickly and easily (and often freely). McDonough et al. (2022) showed that no single speleothem proxy could reliably identify a past fire, and it was only through principal component analyses that past fire frequency could be reconstructed. Recent advances in analytical methods for mineral magnetism has potential to enable the development of a novel fire proxy at comparable or greater resolution to those presented in this review. Similarly, refinements to the analyses of biomarkers in speleothems may allow for better quantification of polycyclic aromatic hydrocarbons in speleothems.

$\delta^{18}\text{O}$  in both dripwater and calcite can be impacted by fire events, although the sign of that impact varies.  $\delta^{18}\text{O}$  values have been shown to shift higher in some instances while lower in others, depending on the extent of evaporation of soil stores, the isotopic value of recharging rainfall, whether hydrological pathways were altered to allow for more efficient infiltration, and whether post-fire evaporation rates were enhanced by loss of shade cover (Bian et al., 2019; McDonough et al., 2022; Nagra et al., 2016). This has implications for the interpretation of speleothem  $\delta^{18}\text{O}$  records. The SISAL V2 database is the largest database of speleothem  $\delta^{18}\text{O}$  and  $\delta^{13}\text{C}$  data, with 691 speleothem records from 294 cave sites (Comas-Bru et al., 2020). Between November 2000 and May 2021, ~50% of the SISAL V2 sites experienced at least one fire (when comparing overlap of sites with aggregated MODIS Burned Area data; Figure 10). This represents a significant proportion of the publicly available stalagmite  $\delta^{18}\text{O}$  datasets, and researchers should consider potential fire impacts when interpreting the speleothem  $\delta^{18}\text{O}$  record for both existing and new stalagmite proxy data. The extent of potential fire impacts on calcite  $\delta^{18}\text{O}$  may be quantified through comparison with other hydroclimate proxies that are unaffected by fire (e.g., Sr), or by comparing with  $\delta^{18}\text{O}$  records from nearby deeper caves.

The SISAL V2 database also offers an opportunity for researchers interested in speleothem palaeofire reconstructions. The full suite of data and metadata in the database (including  $\delta^{18}\text{O}$  and  $\delta^{13}\text{C}$  data, dates, age models, location, cave depth, whether there are annual laminae, etc.) may allow for suitable samples to be identified, i.e., shallow caves in fire susceptible regions and for recently formed stalagmites, because using sites known to have recorded at least one fire in the satellite era as a site-specific calibration is likely to be important. By way of inclusion in the SISAL V2 database, datasets are readily available that could be built



upon by use of elemental mapping and petrographic analyses on targeted areas of the records where shifts in stable isotopes might suggest a fire was involved.

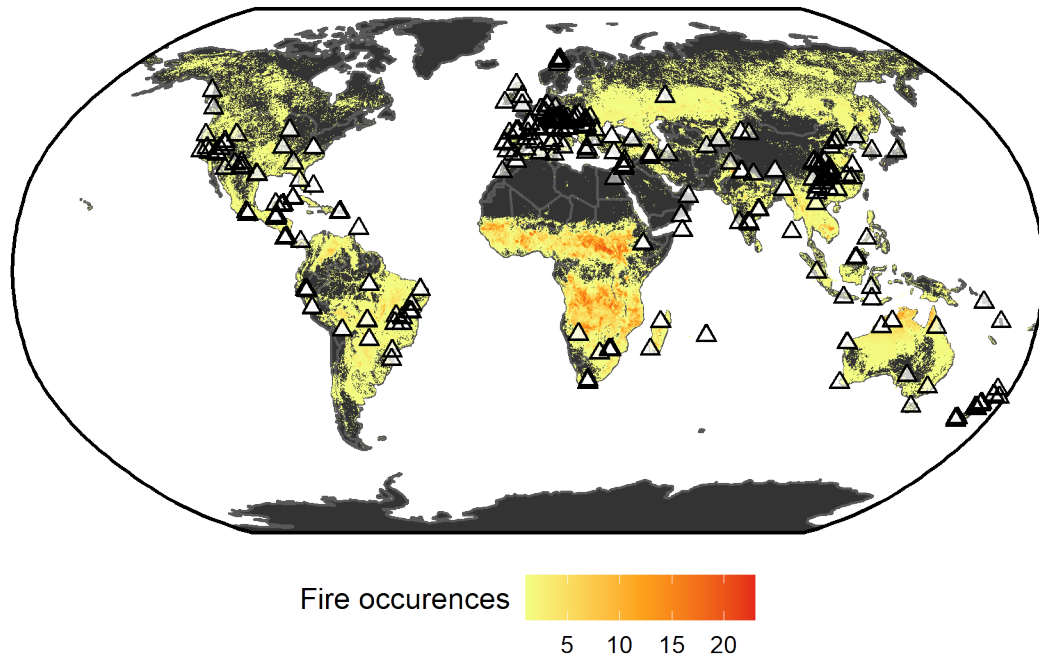


**Figure 10** Samples from the SISAL V2 database (Comas-Bru et al., 2020) plotted against aggregated monthly MODIS Burned Area data (Giglio et al., 2015) for the period November 2000 to May 2021. MODIS data were compiled using Google Earth Engine.

McDonough et al. (2022) showed that not all trace metals contributed similarly to their ‘fire’ principal component during each fire event. They proposed that high peaks could be found where multiple metals loaded on the principal component. This could be achieved during, for example, a ‘moderate’ fire where a lot of material was mobilised, but temperatures were not high enough for those metals to be volatilised (Bodí et al., 2014; McDonough et al., 2022; Figure 4). Conversely, a very intense fire event might produce a smaller peak, as metals volatilised and therefore did not load on the principal component. To investigate this, future work should aim to test this hypothesis by analysing coeval stalagmites which experienced different fires of different fire severities. Being able to reconstruct past fire severity would be a significant outcome for both speleothem palaeoclimatologists and the broader palaeoclimate community, as reconstructing past fire severity is challenging and generally inferred from charcoal abundance and pollen assemblages (Minckley and Long, 2016).

This review has demonstrated that discrete horizons of highly enriched metals (such as iron and zinc) are the ‘smoking gun’ for fire events. Case studies presenting S- $\mu$ XRF maps have demonstrated that these event horizons are clearly visible, and have shown that ash is a likely source. These metals are insoluble and will only be transported through the soil and epikarst when chelated (likely organically bound). While the evidence is strong that these layers are caused by wildfires (i.e. they have been chronologically tied to known fire events) major precipitation events could produce a similar effect by washing in soil organic matter. This effect has been demonstrated in dripwaters (Hartland et al., 2012) and in speleothem calcite (Borsato et al., 2007; Fairchild et al., 2010; Wynn et al., 2014). More research is needed to separate the soil

organic matter metal signal from the wildfire ash metal signal. Further proxy development and validation is needed to determine whether and how  $\delta^{13}\text{C}$  and  $^{14}\text{C}$  are impacted by wildfires. It has been demonstrated that soil microbial communities are affected by wildfires, and that soil  $\text{CO}_2$  can take >5 years post-wildfire to recover (Coleborn et al., 2016b). It follows that speleothem  $\delta^{13}\text{C}$  and  $^{14}\text{C}$  may also be impacted by wildfire, but this effect has yet to be shown. Similarly, high-resolution mineral magnetism is a promising new speleothem proxy, although the applications for palaeofire reconstruction have yet to be fully explored.

As fire regimes are a function of human activity, climate, and vegetation composition, and since speleothems can produce very long, high-resolution, precisely-dated palaeoclimate datasets, they have perhaps unmatched potential to investigate the transition from ‘unmanaged’ fire regimes to ‘managed’ fire regimes when both early and modern humans migrated and started managing landscapes. Speleothems have already been used to investigate the climatic conditions governing early hominin migration (El-Shenawy et al., 2018; Orland et al., 2019), and adding palaeofire would be a natural extension of that research. This research would be of significant importance to our understanding of those early peoples, their use of fire, and how ecosystems changed with their arrival. Resulting research would be of global interest and significance as it could help to pinpoint the arrival time of early hominins (and their successors), and further elucidate the relationship between climate, human activity, and vegetation which comprises fire regimes. This research would also allow the transition from Indigenous to colonial land management practices to be better understood, and could provide important lessons about best practice land management. This research would be truly multi-disciplinary, and appeal to archaeologists, hydrologists, climatologists, and ecologists.

## Acknowledgments

This review was funded by the Australian Research Council (DP200100203 and LP130100177). NK was supported by an Honours Scholarship from the Australian Institute of Nuclear Science and Engineering (ALNSTU21014). We thank WA Parks and Wildlife staff for enthusiastic assistance in the collection of ash. S- $\mu\text{XRF}$  analyses were undertaken on the XFM beamline at the Australian Synchrotron, part of ANSTO, with thanks to David Patterson. Thanks to Henri Wong and Chris Vardanega at ANSTO ITNS for analyses of ash leachates. Mass spectrometric results were obtained at the Bioanalytical Mass Spectrometry Facility within the Mark Wainwright Analytical Centre of the University of New South Wales, with thanks to Lewis Adler. The authors respectfully acknowledge both the Whadjuk Noongar and Wadandi Noongar peoples as the traditional and spiritual custodians of the Yanchep (on Whadjuk Noongar boodja) and Margaret River (on Wadandi boodja) regions of Western Australia, which are the sites for all case studies presented in Section 6.

## Open Research

Data for case studies 6.1, 6.2, and 6.4 are available at 10.6084/m9.figshare.20289540 (Campbell et al. 2022) (temporary link until data are published <https://figshare.com/s/04ac226c54e8b93ff98e>). Data for case study 6.3 is available with the original publication (McDonough et al., 2022). R and Google Earth Engine scripts to produce Figures 5, 6, 9 and 10 are also included in the data archive at the above DOI.

## References

- Abatzoglou, J.T., Williams, A.P., 2016. Impact of anthropogenic climate change on wildfire across western US forests. *Proc. Natl. Acad. Sci.* 113, 11770–11775. <https://doi.org/10.1073/pnas.1607171113>
- Abatzoglou, J.T., Williams, A.P., Barbero, R., 2019. Global Emergence of Anthropogenic Climate Change in Fire Weather Indices. *Geophys. Res. Lett.* 46, 326–336. <https://doi.org/10.1029/2018GL080959>
- Abbott, I., 2002. Historical records of Noongar fires, 1658-1888: a compendium. Department of Conservation & Land Management, Kensington, WA.
- Abram, N.J., Henley, B.J., Sen Gupta, A., Lippmann, T.J.R., Clarke, H., Dowdy, A.J., Sharples, J.J., Nolan, R.H., Zhang, T., Wooster, M.J., Wurtzel, J.B., Meissner, K.J., Pitman, A.J., Ukkola, A.M., Murphy, B.P., Tapper, N.J., Boer, M.M., 2021. Connections of climate change and variability to large and extreme forest fires in southeast Australia. *Commun. Earth Environ.* 2, 8. <https://doi.org/10.1038/s43247-020-00065-8>
- Alriksson, A., Eriksson, H.M., 1998. Variations in mineral nutrient and C distribution in the soil and vegetation compartments of five temperate tree species in NE Sweden. *For. Ecol. Manag.* 108, 261–273. [https://doi.org/10.1016/S0378-1127\(98\)00230-8](https://doi.org/10.1016/S0378-1127(98)00230-8)
- Appelo, C.A.J., Postma, D., Appelo, C.A.J., Postma, D., 2005. *Geochemistry, Groundwater and Pollution*, 2nd ed. CRC Press, London. <https://doi.org/10.1201/9781439833544>
- Argiriadis, E., Denniston, R.F., Barbante, C., 2019. Improved Polycyclic Aromatic Hydrocarbon and n-Alkane Determination in Speleothems through Cleanroom Sample Processing. *Anal. Chem.* 91, 7007–7011. <https://doi.org/10.1021/acs.analchem.9b00767>
- Ashe, B., McAneney, K.J., Pitman, A.J., 2009. Total cost of fire in Australia. *J. Risk Res.* 12, 121–136. <https://doi.org/10.1080/13669870802648528>
- Baker, A., Blyth, A.J., Jex, C.N., McDonald, J.A., Woltering, M., Khan, S.J., 2019. Glycerol dialkyl glycerol tetraethers (GDGT) distributions from soil to cave: Refining the speleothem paleothermometer. *Org. Geochem.* 136, 103890. <https://doi.org/10.1016/j.orggeochem.2019.06.011>
- Baker, A., Mariethoz, G., Comas-Bru, L., Hartmann, A., Frisia, S., Borsato, A., Treble, P.C., Asrat, A., 2021. The Properties of Annually Laminated Stalagmites-A Global Synthesis. *Rev. Geophys.* 59. <https://doi.org/10.1029/2020RG000722>
- Baldini, J.U.L., Lechleitner, F.A., Breitenbach, S.F.M., van Hunen, J., Baldini, L.M., Wynn, P.M., Jamieson, R.A., Ridley, H.E., Baker, A.J., Walczak, I.W., Fohlmeister, J., 2021. Detecting and quantifying palaeoseasonality in stalagmites using geochemical and modelling approaches. *Quat. Sci. Rev.* 254, 106784. <https://doi.org/10.1016/j.quascirev.2020.106784>

- 1165 Balfour, V.N., Woods, S.W., 2013. The hydrological properties and the effects of hydration on  
1166 vegetative ash from the Northern Rockies, USA. *CATENA* 111, 9–24.  
1167 <https://doi.org/10.1016/j.catena.2013.06.014>
- 1168 Bárcenas-Moreno, G., Bååth, E., 2009. Bacterial and fungal growth in soil heated at different  
1169 temperatures to simulate a range of fire intensities. *Soil Biol. Biochem.* 41, 2517–2526.  
1170 <https://doi.org/10.1016/j.soilbio.2009.09.010>
- 1171 Battistel, D., Kehrwald, N.M., Zennaro, P., Pellegrino, G., Barbaro, E., Zangrando, R., Pedeli,  
1172 X.X., Varin, C., Spolaor, A., Vallelonga, P.T., Gambaro, A., Barbante, C., 2018. High-latitude  
1173 Southern Hemisphere fire history during the mid- to late Holocene (6000–7500 BP).  
1174 *Clim. Past* 14, 871–886. <https://doi.org/10.5194/cp-14-871-2018>
- 1175 Benington, F., Melton, C., Watson, P.J., 1962. Carbon Dating Prehistoric Soot from Salts Cave,  
1176 Kentucky. *Am. Antiq.* 28, 238–241. <https://doi.org/10.2307/278384>
- 1177 Bhattarai, H., Saikawa, E., Wan, X., Zhu, H., Ram, K., Gao, S., Kang, S., Zhang, Q., Zhang, Y.,  
1178 Wu, G., Wang, X., Kawamura, K., Fu, P., Cong, Z., 2019. Levoglucosan as a tracer of biomass  
1179 burning: Recent progress and perspectives. *Atmospheric Res.* 220, 20–33.  
1180 <https://doi.org/10.1016/j.atmosres.2019.01.004>
- 1181 Bian, F., Coleborn, K., Flemons, I., Baker, Andy, Treble, P.C., Hughes, C.E., Baker, Andrew,  
1182 Andersen, M.S., Tozer, M.G., Duan, W., Fogwill, C.J., Fairchild, I.J., 2019. Hydrological and  
1183 geochemical responses of fire in a shallow cave system. *Sci. Total Environ.* 662, 180–191.  
1184 <https://doi.org/10.1016/j.scitotenv.2019.01.102>
- 1185 Blyth, A.J., Hartland, A., Baker, A., 2016. Organic proxies in speleothems – New developments,  
1186 advantages and limitations. *Quat. Sci. Rev.* 149, 1–17.  
1187 <https://doi.org/10.1016/j.quascirev.2016.07.001>
- 1188 Bodí, M.B., Doerr, S.H., Cerdà, A., Mataix-Solera, J., 2012. Hydrological effects of a layer of  
1189 vegetation ash on underlying wettable and water repellent soil. *Geoderma*, Fire effects on soil  
1190 properties 191, 14–23. <https://doi.org/10.1016/j.geoderma.2012.01.006>
- 1191 Bodí, M.B., Martin, D.A., Balfour, V.N., Santín, C., Doerr, S.H., Pereira, P., Cerdà, A., Mataix-  
1192 Solera, J., 2014. Wildland fire ash: Production, composition and eco-hydro-geomorphic effects.  
1193 *Earth-Sci. Rev.* 130, 103–127. <https://doi.org/10.1016/j.earscirev.2013.12.007>
- 1194 BOM, CSIRO, 2020. State of the Climate 2020. corporateName=Bureau of Meteorology.
- 1195 Borsato, A., Frisia, S., Fairchild, I.J., Somogyi, A., Susini, J., 2007. Trace element distribution in  
1196 annual stalagmite laminae mapped by micrometer-resolution X-ray fluorescence: Implications  
1197 for incorporation of environmentally significant species. *Geochim. Cosmochim. Acta* 71, 1494–  
1198 1512. <https://doi.org/10.1016/j.gca.2006.12.016>

- 1199 Borsato, A., Frisia, S., Howard, D., Greig, A., 2021. A guide to synchrotron hard X-ray  
1200 fluorescence mapping of annually laminated stalagmites: Sample preparation, analysis and  
1201 evaluation. *Spectrochim. Acta Part B At. Spectrosc.* 185, 106308.  
1202 <https://doi.org/10.1016/j.sab.2021.106308>
- 1203 Borsato, A., Frisia, S., Wynn, P.M., Fairchild, I.J., Miorandi, R., 2015. Sulphate concentration in  
1204 cave dripwater and speleothems: long-term trends and overview of its significance as proxy for  
1205 environmental processes and climate changes. *Quat. Sci. Rev., Novel approaches to and new*  
1206 *insights from speleothem-based climate reconstructions* 127, 48–60.  
1207 <https://doi.org/10.1016/j.quascirev.2015.05.016>
- 1208 Bowman, D.M.J.S., Balch, J.K., Artaxo, P., Bond, W.J., Carlson, J.M., Cochrane, M.A.,  
1209 D’Antonio, C.M., DeFries, R.S., Doyle, J.C., Harrison, S.P., Johnston, F.H., Keeley, J.E.,  
1210 Krawchuk, M.A., Kull, C.A., Marston, J.B., Moritz, M.A., Prentice, I.C., Roos, C.I., Scott, A.C.,  
1211 Swetnam, T.W., van der Werf, G.R., Pyne, S.J., 2009. Fire in the Earth System. *Science* 324,  
1212 481–484. <https://doi.org/10.1126/science.1163886>
- 1213 Bradley, C., Baker, A., Jex, C.N., Leng, M.J., 2010. Hydrological uncertainties in the modelling  
1214 of cave drip-water  $\delta^{18}\text{O}$  and the implications for stalagmite palaeoclimate reconstructions.  
1215 *Quat. Sci. Rev.* 29, 2201–2214. <https://doi.org/10.1016/j.quascirev.2010.05.017>
- 1216 Brittingham, A., Hren, M.T., Hartman, G., Wilkinson, K.N., Mallol, C., Gasparyan, B., Adler,  
1217 D.S., 2019. Geochemical Evidence for the Control of Fire by Middle Palaeolithic Hominins. *Sci.*  
1218 *Rep.* 9, 15368. <https://doi.org/10.1038/s41598-019-51433-0>
- 1219 Brown, P.M., Kaufmann, M.R., Shepperd, W.D., 1999. Long-term, landscape patterns of past  
1220 fire events in a montane ponderosa pine forest of central Colorado. *Landsc. Ecol.* 14, 513–532.  
1221 <https://doi.org/10.1023/A:1008137005355>
- 1222 Brücher, T., Brovkin, V., Kloster, S., Marlon, J.R., Power, M.J., 2014. Comparing modelled fire  
1223 dynamics with charcoal records for the Holocene. *Clim. Past* 10, 811–824.  
1224 <https://doi.org/10.5194/cp-10-811-2014>
- 1225 Bryant, R.A., Waters, E., Gibbs, L., Gallagher, H.C., Pattison, P., Lusher, D., MacDougall, C.,  
1226 Harms, L., Block, K., Snowdon, E., Sinnott, V., Ireton, G., Richardson, J., Forbes, D., 2014.  
1227 Psychological outcomes following the Victorian Black Saturday bushfires. *Aust. N. Z. J.*  
1228 *Psychiatry* 48, 634–643. <https://doi.org/10.1177/0004867414534476>
- 1229 Buckles, J., Rowe, H.D., 2016. Development and optimization of microbeam X-ray fluorescence  
1230 analysis of Sr in speleothems. *Chem. Geol.* 426, 28–32.  
1231 <https://doi.org/10.1016/j.chemgeo.2016.02.003>
- 1232 Buckley, T.N., Turnbull, T.L., Pfautsch, S., Gharun, M., Adams, M.A., 2012. Differences in water  
1233 use between mature and post-fire regrowth stands of subalpine *Eucalyptus delegatensis* R.  
1234 Baker. *For. Ecol. Manag.* 270, 1–10. <https://doi.org/10.1016/j.foreco.2012.01.008>

- 1235 Campbell, M. et al. (2022) ‘Speleothems as archives for palaeofire proxies’. Figshare. Available  
1236 at: <https://figshare.com/s/04ac226c54e8b93ff98e>.
- 1237 Canadell, J.G., Meyer, C.P. (Mick), Cook, G.D., Dowdy, A., Briggs, P.R., Knauer, J., Pepler, A.,  
1238 Haverd, V., 2021. Multi-decadal increase of forest burned area in Australia is linked to climate  
1239 change. *Nat. Commun.* 12, 6921. <https://doi.org/10.1038/s41467-021-27225-4>
- 1240 Cerrato, J.M., Blake, J.M., Hirani, C., Clark, A.L., Ali, A.-M.S., Artyushkova, K., Peterson, E.,  
1241 Bixby, R.J., 2016. Wildfires and water chemistry: effect of metals associated with wood ash.  
1242 *Environ. Sci. Process. Impacts* 18, 1078–1089. <https://doi.org/10.1039/C6EM00123H>
- 1243 Certini, G., 2005. Effects of fire on properties of forest soils: a review. *Oecologia* 143, 1–10.  
1244 <https://doi.org/10.1007/s00442-004-1788-8>
- 1245 Chapin, F.S., Matson, P.A., Vitousek, P.M., 2011. *Principles of Terrestrial Ecosystem Ecology*.  
1246 Springer New York, New York, NY. <https://doi.org/10.1007/978-1-4419-9504-9>
- 1247 Chen, S., Hoffmann, S.S., Lund, D.C., Cobb, K.M., Emile-Geay, J., Adkins, J.F., 2016. A high-  
1248 resolution speleothem record of western equatorial Pacific rainfall: Implications for Holocene  
1249 ENSO evolution. *Earth Planet. Sci. Lett.* 442, 61–71.  
1250 <https://doi.org/10.1016/j.epsl.2016.02.050>
- 1251 Cheng, H., Edwards, R.L., Hoff, J., Gallup, C.D., Richards, D.A., Asmerom, Y., 2000. The half-  
1252 lives of uranium-234 and thorium-230. *Chem. Geol.* 169, 17–33.  
1253 [https://doi.org/10.1016/S0009-2541\(99\)00157-6](https://doi.org/10.1016/S0009-2541(99)00157-6)
- 1254 Cheng, H., Edwards, R.L., Sinha, A., Spötl, C., Yi, L., Chen, S., Kelly, M., Kathayat, G., Wang, X.,  
1255 Li, X., Kong, X., Wang, Y., Ning, Y., Zhang, H., 2016. The Asian monsoon over the past 640,000  
1256 years and ice age terminations. *Nature* 534, 640–646. <https://doi.org/10.1038/nature18591>
- 1257 Clifford, D.A., Chen, S.-S., Reznik, C., 1993. Volatilizing toxic metals from soil. *Waste Manag.*,  
1258 1993 Symposium on emerging technologies 13, 467–479. [https://doi.org/10.1016/0956-](https://doi.org/10.1016/0956-053X(93)90078-B)  
1259 [053X\(93\)90078-B](https://doi.org/10.1016/0956-053X(93)90078-B)
- 1260 Coleborn, K., 2020. Developing a new proxy for speleothem paleofire records (PhD Thesis).  
1261 University of New South Wales, Australia.
- 1262 Coleborn, K., Baker, Andy, Treble, P.C., Andersen, M.S., Baker, Andrew, Tadros, C.V., Tozer, M.,  
1263 Fairchild, I.J., Spate, A., Meehan, S., 2019. Corrigendum to “The impact of fire on the  
1264 geochemistry of speleothem-forming drip water in a sub-alpine cave” [*Sci. Total Environ.* (2018)  
1265 408–420]. *Sci. Total Environ.* 668, 1339–1340.  
1266 <https://doi.org/10.1016/j.scitotenv.2019.02.350>
- 1267 Coleborn, K., Baker, Andy, Treble, P.C., Andersen, M.S., Baker, Andrew, Tadros, C.V., Tozer, M.,  
1268 Fairchild, I.J., Spate, A., Meehan, S., 2018. The impact of fire on the geochemistry of

- speleothem-forming drip water in a sub-alpine cave. *Sci. Total Environ.* 642, 408–420.  
<https://doi.org/10.1016/j.scitotenv.2018.05.310>
- Coleborn, K., Rau, G.C., Cuthbert, M.O., Baker, A., Navarre, O., 2016a. Solar-forced diurnal regulation of cave drip rates via phreatophyte evapotranspiration. *Hydrol. Earth Syst. Sci.* 20, 4439–4455. <https://doi.org/10.5194/hess-20-4439-2016>
- Coleborn, K., Spate, A., Tozer, M., Andersen, M.S., Fairchild, I.J., MacKenzie, B., Treble, P.C., Meehan, S., Baker, Andrew, Baker, Andy, 2016b. Effects of wildfire on long-term soil CO<sub>2</sub> concentration: implications for karst processes. *Environ. Earth Sci.* 75, 330.  
<https://doi.org/10.1007/s12665-015-4874-9>
- Comas-Bru, L., Rehfeld, K., Roesch, C., Amirnezhad-Mozhdehi, S., Harrison, S.P., Atsawawaranunt, K., Ahmad, S.M., Brahim, Y.A., Baker, A., Bosomworth, M., Breitenbach, S.F.M., Burstyn, Y., Columbu, A., Deininger, M., Demény, A., Dixon, B., Fohlmeister, J., Hatvani, I.G., Hu, J., Kaushal, N., Kern, Z., Labuhn, I., Lechleitner, F.A., Lorrey, A., Martrat, B., Novello, V.F., Oster, J., Pérez-Mejías, C., Scholz, D., Scroxton, N., Sinha, N., Ward, B.M., Warken, S., Zhang, H., SISAL Working Group members, 2020. SISALv2: a comprehensive speleothem isotope database with multiple age–depth models. *Earth Syst. Sci. Data* 12, 2579–2606. <https://doi.org/10.5194/essd-12-2579-2020>
- Constantine, M., Mooney, S., Hibbert, B., Marjo, C., Bird, M., Cohen, T., Forbes, M., McBeath, A., Rich, A., Stride, J., 2021. Using charcoal, ATR FTIR and chemometrics to model the intensity of pyrolysis: Exploratory steps towards characterising fire events. *Sci. Total Environ.* 783, 147052. <https://doi.org/10.1016/j.scitotenv.2021.147052>
- Dahm, C.N., Candelaria-Ley, R.I., Reale, C.S., Reale, J.K., Van Horn, D.J., 2015. Extreme water quality degradation following a catastrophic forest fire. *Freshw. Biol.* 60, 2584–2599.  
<https://doi.org/10.1111/fwb.12548>
- Denis, E.H., Toney, J.L., Tarozo, R., Scott Anderson, R., Roach, L.D., Huang, Y., 2012. Polycyclic aromatic hydrocarbons (PAHs) in lake sediments record historic fire events: Validation using HPLC-fluorescence detection. *Org. Geochem.* 45, 7–17.  
<https://doi.org/10.1016/j.orggeochem.2012.01.005>
- Di Virgilio, G., Evans, J.P., Blake, S.A.P., Armstrong, M., Dowdy, A.J., Sharples, J., McRae, R., 2019. Climate Change Increases the Potential for Extreme Wildfires. *Geophys. Res. Lett.* 46, 8517–8526. <https://doi.org/10.1029/2019GL083699>
- Dredge, J., 2014. Aerosol contributions to speleothem geochemistry (d<sub>ph</sub>). University of Birmingham.
- Dreybrodt, W., 1999. Chemical kinetics, speleothem growth and climate. *Boreas* 28, 347–356.  
<https://doi.org/10.1111/j.1502-3885.1999.tb00224.x>

- Drysdale, R., Couchoud, I., Zanchetta, G., Isola, I., Regattieri, E., Hellstrom, J., Govin, A., Tzedakis, P.C., Ireland, T., Corrick, E., Greig, A., Wong, H., Piccini, L., Holden, P., Woodhead, J., 2020. Magnesium in subaqueous speleothems as a potential palaeotemperature proxy. *Nat. Commun.* 11, 5027. <https://doi.org/10.1038/s41467-020-18083-7>
- Dutta, R., Das, A., Aryal, J., 2016. Big data integration shows Australian bush-fire frequency is increasing significantly. *R. Soc. Open Sci.* 3, 150241. <https://doi.org/10.1098/rsos.150241>
- Eichler, A., Tinner, W., Brüttsch, S., Olivier, S., Papina, T., Schwikowski, M., 2011. An ice-core based history of Siberian forest fires since AD 1250. *Quat. Sci. Rev.* 30, 1027–1034. <https://doi.org/10.1016/j.quascirev.2011.02.007>
- El-Shenawy, M.I., Kim, S.-T., Schwarcz, H.P., Asmerom, Y., Polyak, V.J., 2018. Speleothem evidence for the greening of the Sahara and its implications for the early human dispersal out of sub-Saharan Africa. *Quat. Sci. Rev.* 188, 67–76. <https://doi.org/10.1016/j.quascirev.2018.03.016>
- Escudey, M., Fuente, P. de la, Antilén, M., Molina, M., Escudey, M., Fuente, P. de la, Antilén, M., Molina, M., 2010. Effect of ash from forest fires on phosphorus availability, transport, chemical forms, and content in volcanic soils. *Environ. Chem.* 7, 103–110. <https://doi.org/10.1071/EN09067>
- Etiegni, L., Campbell, A.G., Mahler, R.L., 1991. Evaluation of wood ash disposal on agricultural land. I. Potential as a soil additive and liming agent. *Commun. Soil Sci. Plant Anal.* 22, 243–256. <https://doi.org/10.1080/00103629109368412>
- Fairchild, I., Spötl, C., Frisia, S., Borsato, A., Susini, J., Wynn, P., Cauzid, J., 2010. Petrology and geochemistry of annually laminated stalagmites from an Alpine cave (Obir, Austria): Seasonal cave physiology. *Geol. Soc. Lond. Spec. Publ.* 336, 295–321. <https://doi.org/10.1144/SP336.16>
- Fairchild, I.J., Baker, A., 2012. *Speleothem science: from process to past environments*. John Wiley & Sons.
- Fairchild, I.J., Smith, C.L., Baker, A., Fuller, L., Spötl, C., Matthey, D., McDermott, F., E.I.M.F., 2006. Modification and preservation of environmental signals in speleothems. *Earth-Sci. Rev.* 75, 105–153. <https://doi.org/10.1016/j.earscirev.2005.08.003>
- Fairchild, I.J., Treble, P.C., 2009. Trace elements in speleothems as recorders of environmental change. *Quat. Sci. Rev.* 28, 449–468. <https://doi.org/10.1016/j.quascirev.2008.11.007>
- Faraji, M., Borsato, A., Frisia, S., Hellstrom, J.C., Lorrey, A., Hartland, A., Greig, A., Matthey, D.P., 2021. Accurate dating of stalagmites from low seasonal contrast tropical Pacific climate using Sr 2D maps, fabrics and annual hydrological cycles. *Sci. Rep.* 11, 2178. <https://doi.org/10.1038/s41598-021-81941-x>



- Feinberg, J.M., Lascu, I., Lima, E.A., Weiss, B.P., Dorale, J.A., Alexander, E.C., Edwards, R.L., 2020. Magnetic detection of paleoflood layers in stalagmites and implications for historical land use changes. *Earth Planet. Sci. Lett.* 530, 115946. <https://doi.org/10.1016/j.epsl.2019.115946>
- Filkov, A.I., Ngo, T., Matthews, S., Telfer, S., Penman, T.D., 2020. Impact of Australia's catastrophic 2019/20 bushfire season on communities and environment. Retrospective analysis and current trends. *J. Saf. Sci. Resil.* 1, 44–56. <https://doi.org/10.1016/j.jnlssr.2020.06.009>
- Fletcher, M.-S., Hall, T., Alexandra, A.N., 2021a. The loss of an indigenous constructed landscape following British invasion of Australia: An insight into the deep human imprint on the Australian landscape. *Ambio* 50, 138–149. <https://doi.org/10.1007/s13280-020-01339-3>
- Fletcher, M.-S., Romano, A., Connor, S., Mariani, M., Maezumi, S.Y., 2021b. Catastrophic Bushfires, Indigenous Fire Knowledge and Reframing Science in Southeast Australia. *Fire* 4, 61. <https://doi.org/10.3390/fire4030061>
- Fohlmeister, J., 2012. A statistical approach to construct composite climate records of dated archives. *Quat. Geochronol.* 14, 48–56. <https://doi.org/10.1016/j.quageo.2012.06.007>
- Frisia, S., 2014. Microstratigraphic logging of calcite fabrics in speleothems as tool for palaeoclimate studies. *Int. J. Speleol.* 44. <https://doi.org/10.5038/1827-806X.44.1.1>
- Frisia, S., Borsato, A., 2010. Chapter 6 Karst, in: Alonso-Zarza, A.M., Tanner, L.H. (Eds.), *Developments in Sedimentology, Carbonates in Continental Settings: Facies, Environments, and Processes*. Elsevier, pp. 269–318. [https://doi.org/10.1016/S0070-4571\(09\)06106-8](https://doi.org/10.1016/S0070-4571(09)06106-8)
- Frisia, S., Borsato, A., Fairchild, I.J., Susini, J., 2005. Variations in atmospheric sulphate recorded in stalagmites by synchrotron micro-XRF and XANES analyses. *Earth Planet. Sci. Lett.* 235, 729–740. <https://doi.org/10.1016/j.epsl.2005.03.026>
- Frisia, S., Borsato, A., Susini, J., 2008. Synchrotron radiation applications to past volcanism archived in speleothems: An overview. *J. Volcanol. Geotherm. Res., Explosive volcanism in the central Mediterranean area during the late Quaternary - linking sources and distal archives* 177, 96–100. <https://doi.org/10.1016/j.jvolgeores.2007.11.010>
- Fu, R.R., Hess, K., Jaqueto, P., Novello, V.F., Kukla, T., Trindade, R.I.F., Stríkis, N.M., Cruz, F.W., Ben Dor, O., 2021. High-Resolution Environmental Magnetism Using the Quantum Diamond Microscope (QDM): Application to a Tropical Speleothem. *Front. Earth Sci.* 8.
- Gázquez, F., Calaforra, J.M., Forti, P., 2011. Black Mn-Fe Crusts as Markers of Abrupt Palaeoenvironmental Changes in El Soplao Cave (Cantabria, Spain). *Int. J. Speleol.* 40, 163–169. <https://doi.org/10.5038/1827-806X.40.2.8>

- 1371 Gedalof, Z., Peterson, D.L., Mantua, N.J., 2005. Atmospheric, Climatic, and Ecological Controls  
1372 on Extreme Wildfire Years in the Northwestern United States. *Ecol. Appl.* 15, 154–174.  
1373 <https://doi.org/10.1890/03-5116>
- 1374 Gedye, S.J., Jones, R.T., Tinner, W., Ammann, B., Oldfield, F., 2000. The use of mineral  
1375 magnetism in the reconstruction of fire history: a case study from Lago di Origlio, Swiss Alps.  
1376 *Palaeogeogr. Palaeoclimatol. Palaeoecol., Fire and the Palaeoenvironment* 164, 101–110.  
1377 [https://doi.org/10.1016/S0031-0182\(00\)00178-4](https://doi.org/10.1016/S0031-0182(00)00178-4)
- 1378 Genty, D., Massault, M., 1999. Carbon transfer dynamics from bomb-14C and d13C time series  
1379 of a laminated stalagmite from SW France—Modelling and comparison with other stalagmite  
1380 records. *Geochim. Cosmochim. Acta* 63, 1537–1548.
- 1381 Giglio, L., Justice, C., Boschetti, L., Roy, D., 2015. MCD64A1 MODIS/Terra+Aqua Burned Area  
1382 Monthly L3 Global 500m SIN Grid V006.
- 1383 Giglio, L., Randerson, J.T., van der Werf, G.R., Kasibhatla, P.S., Collatz, G.J., Morton, D.C.,  
1384 DeFries, R.S., 2010. Assessing variability and long-term trends in burned area by merging  
1385 multiple satellite fire products. *Biogeosciences* 7, 1171–1186. [https://doi.org/10.5194/bg-7-](https://doi.org/10.5194/bg-7-1171-2010)  
1386 [1171-2010](https://doi.org/10.5194/bg-7-1171-2010)
- 1387 Goede, A., McCulloch, M., McDermott, F., Hawkesworth, C., 1998. Aeolian contribution to  
1388 strontium and strontium isotope variations in a Tasmanian speleothem. *Chem. Geol.* 149, 37–  
1389 50. [https://doi.org/10.1016/S0009-2541\(98\)00035-7](https://doi.org/10.1016/S0009-2541(98)00035-7)
- 1390 Gongalsky, K.B., Malmström, A., Zaitsev, A.S., Shakhob, S.V., Bengtsson, J., Persson, T., 2012.  
1391 Do burned areas recover from inside? An experiment with soil fauna in a heterogeneous  
1392 landscape. *Appl. Soil Ecol.* 59, 73–86. <https://doi.org/10.1016/j.apsoil.2012.03.017>
- 1393 Gosling, W.D., Cornelissen, H.L., McMichael, C.N.H., 2019. Reconstructing past fire  
1394 temperatures from ancient charcoal material. *Palaeogeogr. Palaeoclimatol. Palaeoecol.* 520,  
1395 128–137. <https://doi.org/10.1016/j.palaeo.2019.01.029>
- 1396 Gradziński, M., Górny, A., Pazdur, A., Pazdur, M.F., 2003. Origin of black coloured laminae in  
1397 speleothems from the Kraków-Wieluń; Upland, Poland. *Boreas* 32, 532–542.  
1398 <https://doi.org/10.1111/j.1502-3885.2003.tb01233.x>
- 1399 Gradziński, M., Hercman, H., Nowak, M., Bella, P., 2007. Age of Black Coloured Laminae  
1400 Within Speleothems from Domica Cave and Its Significance for Dating of Prehistoric Human  
1401 Settlement. *GEOCHR* 28, 39–45. <https://doi.org/10.2478/v10003-007-0029-7>
- 1402 Granged, Arturo J.P., Jordán, A., Zavala, L.M., Muñoz-Rojas, M., Mataix-Solera, J., 2011. Short-  
1403 term effects of experimental fire for a soil under eucalyptus forest (SE Australia). *Geoderma*  
1404 167–168, 125–134. <https://doi.org/10.1016/j.geoderma.2011.09.011>

- Granged, Arturo J. P., Zavala, L.M., Jordán, A., Bárcenas-Moreno, G., 2011. Post-fire evolution of soil properties and vegetation cover in a Mediterranean heathland after experimental burning: A 3-year study. *Geoderma* 164, 85–94.  
<https://doi.org/10.1016/j.geoderma.2011.05.017>
- Grieman, M.M., Aydin, M., Isaksson, E., Schwikowski, M., Saltzman, E.S., 2018. Aromatic acids in an Arctic ice core from Svalbard: a proxy record of biomass burning. *Clim. Past* 14, 637–651.  
<https://doi.org/10.5194/cp-14-637-2018>
- Griffiths, M.L., Johnson, K.R., Pausata, F.S.R., White, J.C., Henderson, G.M., Wood, C.T., Yang, H., Ersek, V., Conrad, C., Sekhon, N., 2020. End of Green Sahara amplified mid- to late Holocene megadroughts in mainland Southeast Asia. *Nat. Commun.* 11, 4204.  
<https://doi.org/10.1038/s41467-020-17927-6>
- Gruell, G.E., 1985. Fire on the early western landscape: An annotated record of wildland fires 1776–1900. *Northwest Sci.* 59, 97–107.
- Guillong, M., Latkoczy, C., Seo, J.H., Günther, D., Heinrich, C.A., 2008. Determination of sulfur in fluid inclusions by laser ablation ICP-MS. *J. Anal. At. Spectrom.* 23, 1581–1589.  
<https://doi.org/10.1039/B807383J>
- Guo, F., Clemens, S., Liu, X., Long, Y., Li, D., Tan, L., Liu, C., Yan, H., Sun, Y., 2021. Application of XRF Scanning to Different Geological Archives. *Earth Space Sci.* 8, e2020EA001589.  
<https://doi.org/10.1029/2020EA001589>
- Haberle, S.G., David, B., 2004. Climates of change: human dimensions of Holocene environmental change in low latitudes of the PEPHII transect. *Quat. Int., Climates, human, and natural system of the PEPHII transect* 118–119, 165–179. [https://doi.org/10.1016/S1040-6182\(03\)00136-8](https://doi.org/10.1016/S1040-6182(03)00136-8)
- Hageman, P.L., 2007. U.S. Geological Survey Field Leach Test for Assessing Water Reactivity and Leaching Potential of Mine Wastes, Soils, and Other Geologic and Environmental Materials (USGS Numbered Series No. 5-D3), U.S. Geological Survey Field Leach Test for Assessing Water Reactivity and Leaching Potential of Mine Wastes, Soils, and Other Geologic and Environmental Materials, Techniques and Methods. <https://doi.org/10.3133/tm5D3>
- Halas, S., Szaran, J., 2001. Improved thermal decomposition of sulfates to SO<sub>2</sub> and mass spectrometric determination of  $\delta^{34}\text{S}$  of IAEA SO-5, IAEA SO-6 and NBS-127 sulfate standards. *Rapid Commun. Mass Spectrom.* 15, 1618–1620. <https://doi.org/10.1002/rcm.416>
- Hallam, S., 2014. *Fire and Hearth: A study of Aboriginal usage and European usurpation in south-western Australia*. UWA Publishing, Perth.

- Hanan, E.J., Ren, J., Tague, C.L., Kolden, C.A., Abatzoglou, J.T., Bart, R.R., Kennedy, M.C., Liu, M., Adam, J.C., 2021. How climate change and fire exclusion drive wildfire regimes at actionable scales. *Environ. Res. Lett.* 16, 024051. <https://doi.org/10.1088/1748-9326/abd78e>
- Hantson, S., Arneth, A., Harrison, S.P., Kelley, D.I., Prentice, I.C., Rabin, S.S., Archibald, S., Mouillot, F., Arnold, S.R., Artaxo, P., Bachelet, D., Ciais, P., Forrest, M., Friedlingstein, P., Hickler, T., Kaplan, J.O., Kloster, S., Knorr, W., Lasslop, G., Li, F., Mangeon, S., Melton, J.R., Meyn, A., Sitch, S., Spessa, A., van der Werf, G.R., Voulgarakis, A., Yue, C., 2016. The status and challenge of global fire modelling. *Biogeosciences* 13, 3359–3375. <https://doi.org/10.5194/bg-13-3359-2016>
- Harper, A.R., Santin, C., Doerr, S.H., Froyd, C.A., Albini, D., Otero, X.L., Viñas, L., Pérez-Fernández, B., 2019. Chemical composition of wildfire ash produced in contrasting ecosystems and its toxicity to *Daphnia magna*. *Int. J. Wildland Fire* 28, 726. <https://doi.org/10.1071/WF18200>
- Harrison, S.P., Bartlein, P.J., Brewer, S., Prentice, I.C., Boyd, M., Hessler, I., Holmgren, K., Izumi, K., Willis, K., 2014. Climate model benchmarking with glacial and mid-Holocene climates. *Clim. Dyn.* 43, 671–688. <https://doi.org/10.1007/s00382-013-1922-6>
- Hart, S.C., DeLuca, T.H., Newman, G.S., MacKenzie, M.D., Boyle, S.I., 2005. Post-fire vegetative dynamics as drivers of microbial community structure and function in forest soils. *For. Ecol. Manag., Forest Soils Research: Theory, Reality and its Role in Technology* 220, 166–184. <https://doi.org/10.1016/j.foreco.2005.08.012>
- Hartland, A., Adam, Fairchild, I., Lead, J., Dominguezvillar, D., Baker, A., Gunn, J., Baalousha, M., 2010. The dripwaters and speleothems of Poole's Cavern: A review of recent and ongoing research. *Cave Karst Sci.* 36, 37–46.
- Hartland, A., Fairchild, I.J., Lead, J.R., Borsato, A., Baker, A., Frisia, S., Baalousha, M., 2012. From soil to cave: Transport of trace metals by natural organic matter in karst dripwaters. *Chem. Geol.* 304–305, 68–82. <https://doi.org/10.1016/j.chemgeo.2012.01.032>
- Hartland, A., Fairchild, I.J., Lead, J.R., Zhang, H., Baalousha, M., 2011. Size, speciation and lability of NOM–metal complexes in hyperalkaline cave dripwater. *Geochim. Cosmochim. Acta* 75, 7533–7551. <https://doi.org/10.1016/j.gca.2011.09.030>
- Hartland, A., Fairchild, I.J., Müller, W., Dominguez-Villar, D., 2014. Preservation of NOM–metal complexes in a modern hyperalkaline stalagmite: Implications for speleothem trace element geochemistry. *Geochim. Cosmochim. Acta* 128, 29–43. <https://doi.org/10.1016/j.gca.2013.12.005>
- Hawkins, L.R., Abatzoglou, J.T., Li, S., Rupp, D.E., 2022. Anthropogenic Influence on Recent Severe Autumn Fire Weather in the West Coast of the United States. *Geophys. Res. Lett.* 49, e2021GL095496. <https://doi.org/10.1029/2021GL095496>

- HersHKovitz, I., Weber, G.W., Quam, R., Duval, M., Grün, R., Kinsley, L., Ayalon, A., Bar-Matthews, M., Valladas, H., Mercier, N., Arsuaga, J.L., Martín-Torres, M., Castro, J.M.B. de, Fornai, C., Martín-Francés, L., Sarig, R., May, H., Krenn, V.A., Slon, V., Rodríguez, L., García, R., Lorenzo, C., Carretero, J.M., Frumkin, A., Shahack-Gross, R., Mayer, D.E.B.-Y., Cui, Y., Wu, X., Peled, N., Groman-Yaroslavski, I., Weissbrod, L., Yeshurun, R., Tsatskin, A., Zaidner, Y., Weinstein-Evron, M., 2018. The earliest modern humans outside Africa. *Science*.  
<https://doi.org/10.1126/science.aap8369>
- Hope, P., Timbal, B., Fawcett, R., 2010. Associations between rainfall variability in the southwest and southeast of Australia and their evolution through time. *Int. J. Climatol.* 30, 1360–1371. <https://doi.org/10.1002/joc.1964>
- Hua, Q., McDonald, J., Redwood, D., Drysdale, R., Lee, S., Fallon, S., Hellstrom, J., 2012. Robust chronological reconstruction for young speleothems using radiocarbon. *Quat. Geochronol.* 14, 67–80. <https://doi.org/10.1016/j.quageo.2012.04.017>
- Huguet, C., Routh, J., Fietz, S., Lone, M.A., Kalpana, M.S., Ghosh, P., Mangini, A., Kumar, V., Rangarajan, R., 2018. Temperature and Monsoon Tango in a Tropical Stalagmite: Last Glacial-Interglacial Climate Dynamics. *Sci. Rep.* 8, 5386. <https://doi.org/10.1038/s41598-018-23606-w>
- Iglesias, V., Balch, J.K., Travis, W.R., 2022. U.S. fires became larger, more frequent, and more widespread in the 2000s. *Sci. Adv.* 8, eabc0020. <https://doi.org/10.1126/sciadv.abc0020>
- Iglesias, V., Yospin, G.I., Whitlock, C., 2015. Reconstruction of fire regimes through integrated paleoecological proxy data and ecological modeling. *Front. Plant Sci.* 5.  
<https://doi.org/10.3389/fpls.2014.00785>
- Jaffey, A.H., Flynn, K.F., Glendenin, L.E., Bentley, W.C., Essling, A.M., 1971. Precision Measurement of Half-Lives and Specific Activities of  $^{235}\text{U}$  and  $^{238}\text{U}$  *Phys. Rev. C* 4, 1889–1906.  
<https://doi.org/10.1103/PhysRevC.4.1889>
- Jenkins, M., Adams, M.A., 2010. Vegetation type determines heterotrophic respiration in subalpine Australian ecosystems. *Glob. Change Biol.* 16, 209–219.  
<https://doi.org/10.1111/j.1365-2486.2009.01954.x>
- Jex, C.N., Pate, G.H., Blyth, A.J., Spencer, R.G., Hernes, P.J., Khan, S.J., Baker, A., 2014. Lignin biogeochemistry: from modern processes to Quaternary archives. *Quat. Sci. Rev.* 87, 46–59.
- Jones, M.W., Abatzoglou, J.T., Veraverbeke, S., Andela, N., Lasslop, G., Forkel, M., Smith, A.J.P., Burton, C., Betts, R.A., van der Werf, G.R., Sitch, S., Canadell, J.G., Santín, C., Kolden, C., Doerr, S.H., Le Quéré, C., 2022. Global and regional trends and drivers of fire under climate change. *Rev. Geophys.* n/a, e2020RG000726. <https://doi.org/10.1029/2020RG000726>

- Kaal, J., Martínez-Pillado, V., Cortizas, A.M., Sánchez, J.S., Aranburu, A., Arsuaga, J.-L., Iriarte, E., 2021. Bacteria, guano and soot: Source assessment of organic matter preserved in black laminae in stalagmites from caves of the Sierra de Atapuerca (N Spain). *Int. J. Speleol.* 50. <https://doi.org/10.5038/1827-806X.50.2.2382>
- Keeley, J.E., 2009. Fire intensity, fire severity and burn severity: a brief review and suggested usage. *Int. J. Wildland Fire* 18, 116–126. <https://doi.org/10.1071/WF07049>
- Kehrwald, N.M., Aleman, J., Coughlan, M., Courtney-Mustaphi, C., Githumbi, E., Magi, B., Marlon, J., Power, M.J., 2016. One thousand years of fires: Integrating proxy and model data. *Front. Biogeogr.* 8. <https://doi.org/10.21425/F5FBG29606>
- Kemperl, J., Maček, J., 2009. Precipitation of calcium carbonate from hydrated lime of variable reactivity, granulation and optical properties. *Int. J. Miner. Process.* 93, 84–88. <https://doi.org/10.1016/j.minpro.2009.05.006>
- Khanna, P.K., Raison, R.J., Falkiner, R.A., 1994. Chemical properties of ash derived from Eucalyptus litter and its effects on forest soils. *For. Ecol. Manag., Ameliorative practices for restoring and maintaining* 66, 107–125. [https://doi.org/10.1016/0378-1127\(94\)90151-1](https://doi.org/10.1016/0378-1127(94)90151-1)
- Lachniet, M.S., 2009. Climatic and environmental controls on speleothem oxygen-isotope values. *Quat. Sci. Rev.* 28, 412–432. <https://doi.org/10.1016/j.quascirev.2008.10.021>
- Lascu, I., Feinberg, J.M., Dorale, J.A., Cheng, H., Edwards, R.L., 2016. Age of the Laschamp excursion determined by U-Th dating of a speleothem geomagnetic record from North America. *Geology* 44, 139–142. <https://doi.org/10.1130/G37490.1>
- Lechleitner, F.A., Fohlmeister, J., McIntyre, C., Baldini, L.M., Jamieson, R.A., Hercman, H., Gąsiorowski, M., Pawlak, J., Stefaniak, K., Socha, P., Eglinton, T.I., Baldini, J.U.L., 2016. A novel approach for construction of radiocarbon-based chronologies for speleothems. *Quat. Geochronol.* 35, 54–66. <https://doi.org/10.1016/j.quageo.2016.05.006>
- Legrand, M., McConnell, J., Fischer, H., Wolff, E.W., Preunkert, S., Arienzo, M., Chellman, N., Leuenberger, D., Maselli, O., Place, P., Sigl, M., Schüpbach, S., Flannigan, M., 2016. Boreal fire records in Northern Hemisphere ice cores: a review. *Clim. Past* 12, 2033–2059. <https://doi.org/10.5194/cp-12-2033-2016>
- Li, F., Levis, S., Ward, D.S., 2013. Quantifying the role of fire in the Earth system – Part 1: Improved global fire modeling in the Community Earth System Model (CESM1). *Biogeosciences* 10, 2293–2314. <https://doi.org/10.5194/bg-10-2293-2013>
- Liu, Y., 2018. New development and application needs for Earth system modeling of fire–climate–ecosystem interactions. *Environ. Res. Lett.* 13, 011001. <https://doi.org/10.1088/1748-9326/aaa347>

- 1542 Lowe, M.-A., McGrath, G., Leopold, M., 2021. The Impact of Soil Water Repellency and Slope  
1543 upon Runoff and Erosion. *Soil Tillage Res.* 205, 104756.  
1544 <https://doi.org/10.1016/j.still.2020.104756>
- 1545 Lucas, C., 2010. On developing a historical fire weather data-set for Australia. *Aust. Meteorol.*  
1546 *Oceanogr. J.* 60, 1–14.
- 1547 Makhubela, T.V., Kramers, J.D., 2022. Testing a new combined (U,Th)–He and U/Th dating  
1548 approach on Plio-Pleistocene calcite speleothems. *Quat. Geochronol.* 67, 101234.  
1549 <https://doi.org/10.1016/j.quageo.2021.101234>
- 1550 Mariani, M., Connor, S.E., Theuerkauf, M., Herbert, A., Kuneš, P., Bowman, D., Fletcher, M.-S.,  
1551 Head, L., Kershaw, A.P., Haberle, S.G., Stevenson, J., Adeleye, M., Cadd, H., Hopf, F., Briles, C.,  
1552 2022. Disruption of cultural burning promotes shrub encroachment and unprecedented  
1553 wildfires. *Front. Ecol. Environ.* n/a. <https://doi.org/10.1002/fee.2395>
- 1554 Mariani, M., Fletcher, M.-S., Holz, A., Nyman, P., 2016. ENSO controls interannual fire activity  
1555 in southeast Australia. *Geophys. Res. Lett.* 43, 10,891–10,900.  
1556 <https://doi.org/10.1002/2016GL070572>
- 1557 Markowska, M., Baker, A., Treble, P.C., Andersen, M.S., Hankin, S., Jex, C.N., Tadros, C.V.,  
1558 Roach, R., 2015. Unsaturated zone hydrology and cave drip discharge water response:  
1559 Implications for speleothem paleoclimate record variability. *J. Hydrol., Advances in*  
1560 *Paleohydrology Research and Applications* 529, 662–675.  
1561 <https://doi.org/10.1016/j.jhydrol.2014.12.044>
- 1562 Markowska, M., Fohlmeister, J., Treble, P.C., Baker, A., Andersen, M.S., Hua, Q., 2019.  
1563 Modelling the 14C bomb-pulse in young speleothems using a soil carbon continuum model.  
1564 *Geochim. Cosmochim. Acta* 261, 342–367. <https://doi.org/10.1016/j.gca.2019.04.029>
- 1565 Marlon, J.R., 2020. What the past can say about the present and future of fire. *Quat. Res.* 96,  
1566 66–87. <https://doi.org/10.1017/qua.2020.48>
- 1567 Marlon, J.R., Bartlein, P.J., Gavin, D.G., Long, C.J., Anderson, R.S., Briles, C.E., Colombaroli,  
1568 D., Hallett, D.J., Power, M.J., Scharf, E.A., Walsh, M.K., 2012. Long-term perspective on  
1569 wildfires in the western USA. *Proc. Natl. Acad. Sci.* 109, E535–E543.  
1570 <https://doi.org/10.1073/pnas.1112839109>
- 1571 Marlon, J.R., Kelly, R., Daniau, A.-L., Vannière, B., Power, M.J., Bartlein, P., Higuera, P.,  
1572 Blarquez, O., Brewer, S., Brücher, T., Feurdean, A., Romera, G.G., Iglesias, V., Maezumi, S.Y.,  
1573 Magi, B., Courtney Mustaphi, C.J., Zhihai, T., 2016. Reconstructions of biomass burning from  
1574 sediment-charcoal records to improve data–model comparisons. *Biogeosciences* 13, 3225–  
1575 3244. <https://doi.org/10.5194/bg-13-3225-2016>

- Marty, C., Houle, D., Gagnon, C., Duchesne, L., 2011. Isotopic compositions of S, N and C in soils and vegetation of three forest types in Québec, Canada. *Appl. Geochem.* 26, 2181–2190. <https://doi.org/10.1016/j.apgeochem.2011.08.002>
- May, N., 2022. ‘Disaster’s in the recovery’: bushfire survivors still waiting for homes. *The Guardian*.
- McBride, J.R., 1983. Analysis of Tree Rings and Fire Scars to Establish Fire History.
- McClean, R.G., Kean, W.F., 1993. Contributions of wood ash magnetism to archaeomagnetic properties of fire pits and hearths. *Earth Planet. Sci. Lett.* 119, 387–394. [https://doi.org/10.1016/0012-821X\(93\)90146-Z](https://doi.org/10.1016/0012-821X(93)90146-Z)
- McConnell, J.R., Edwards, R., Kok, G.L., Flanner, M.G., Zender, C.S., Saltzman, E.S., Banta, J.R., Pasteris, D.R., Carter, M.M., Kahl, J.D.W., 2007. 20th-Century Industrial Black Carbon Emissions Altered Arctic Climate Forcing. *Science* 317, 1381–1384. <https://doi.org/10.1126/science.1144856>
- McDonough, L.K., Treble, P.C., Baker, A., Borsato, A., Frisia, S., Nagra, G., Coleborn, K., Gagan, M.K., Zhao, J., Paterson, D., 2022. Past fires and post-fire impacts reconstructed from a southwest Australian stalagmite. *Geochim. Cosmochim. Acta*. <https://doi.org/10.1016/j.gca.2022.03.020>
- McWethy, D.B., Whitlock, C., Wilmshurst, J.M., McGlone, M.S., Fromont, M., Li, X., Dieffenbacher-Krall, A., Hobbs, W.O., Fritz, S.C., Cook, E.R., 2010. Rapid landscape transformation in South Island, New Zealand, following initial Polynesian settlement. *Proc. Natl. Acad. Sci.* 107, 21343–21348. <https://doi.org/10.1073/pnas.1011801107>
- Meng, Q.-B., Wang, C.-K., Liu, J.-F., Zhang, M.-W., Lu, M.-M., Wu, Y., 2020. Physical and micro-structural characteristics of limestone after high temperature exposure. *Bull. Eng. Geol. Environ.* 79, 1259–1274. <https://doi.org/10.1007/s10064-019-01620-0>
- Minckley, T.A., Long, C.J., 2016. Paleofire severity and vegetation change in the Cascade Range, Oregon, USA. *Quat. Res.* 85, 211–217. <https://doi.org/10.1016/j.yqres.2015.12.010>
- Mitchell, S.G., Reiners, P.W., 2003. Influence of wildfires on apatite and zircon (U-Th)/He ages. *Geology* 31, 1025–1028. <https://doi.org/10.1130/G19758.1>
- Molinari, C., Hantson, S., Nieradzik, L.P., 2021. Fire Dynamics in Boreal Forests Over the 20th Century: A Data-Model Comparison. *Front. Ecol. Evol.* 9, 598. <https://doi.org/10.3389/fevo.2021.728958>
- Molinari, C., Lehsten, V., Bradshaw, R.H.W., Power, M.J., Harmand, P., Arneth, A., Kaplan, J.O., Vannière, B., Sykes, M.T., 2013. Exploring potential drivers of European biomass burning over the Holocene: a data-model analysis. *Glob. Ecol. Biogeogr.* 22, 1248–1260. <https://doi.org/10.1111/geb.12090>



- 1611 Mooney, S.D., Harrison, S.P., Bartlein, P.J., Daniau, A.-L., Stevenson, J., Brownlie, K.C.,  
1612 Buckman, S., Cupper, M., Luly, J., Black, M., Colhoun, E., D'Costa, D., Dodson, J., Haberle, S.,  
1613 Hope, G.S., Kershaw, P., Kenyon, C., McKenzie, M., Williams, N., 2011. Late Quaternary fire  
1614 regimes of Australasia. *Quat. Sci. Rev.* 30, 28–46.  
1615 <https://doi.org/10.1016/j.quascirev.2010.10.010>
- 1616 Moropoulou, A., Bakolas, A., Aggelakopoulou, E., 2001. The effects of limestone characteristics  
1617 and calcination temperature to the reactivity of the quicklime. *Cem. Concr. Res.* 31, 633–639.  
1618 [https://doi.org/10.1016/S0008-8846\(00\)00490-7](https://doi.org/10.1016/S0008-8846(00)00490-7)
- 1619 Müller, W., Fietzke, J., 2016. The Role of LA–ICP–MS in Palaeoclimate Research. *Elements* 12,  
1620 329–334. <https://doi.org/10.2113/gselements.12.5.329>
- 1621 Nagra, G., Treble, P.C., Andersen, M.S., Bajo, P., Hellstrom, J., Baker, A., 2017. Dating  
1622 stalagmites in mediterranean climates using annual trace element cycles. *Sci. Rep.* 7, 621.  
1623 <https://doi.org/10.1038/s41598-017-00474-4>
- 1624 Nagra, G., Treble, P.C., Andersen, M.S., Fairchild, I.J., Coleborn, K., Baker, A., 2016. A post-  
1625 wildfire response in cave dripwater chemistry. *Hydrol. Earth Syst. Sci.* 20, 2745–2758.  
1626 <https://doi.org/10.5194/hess-20-2745-2016>
- 1627 Naoto, F., Link to external site, this link will open in a new window, Hirokuni, O., Yusuke, Y.,  
1628 Clark, G., Yuhji, Y., 2021. High spatial resolution magnetic mapping using ultra-high sensitivity  
1629 scanning SQUID microscopy on a speleothem from the Kingdom of Tonga, southern Pacific.  
1630 *Earth Planets Space Online* 73. <http://dx.doi.org/10.1186/s40623-021-01401-8>
- 1631 Neary, D.G., Klopatek, C.C., DeBano, L.F., Ffolliott, P.F., 1999. Fire effects on belowground  
1632 sustainability: a review and synthesis. *For. Ecol. Manag.* 122, 51–71.  
1633 [https://doi.org/10.1016/S0378-1127\(99\)00032-8](https://doi.org/10.1016/S0378-1127(99)00032-8)
- 1634 Nicewonger, M.R., Aydin, M., Prather, M.J., Saltzman, E.S., 2020. Reconstruction of Paleofire  
1635 Emissions Over the Past Millennium From Measurements of Ice Core Acetylene. *Geophys. Res.*  
1636 *Lett.* 47, e2019GL085101. <https://doi.org/10.1029/2019GL085101>
- 1637 O'Donnell, A.J., Cullen, L.E., Lachlan McCaw, W., Boer, M.M., Grierson, P.F., 2010.  
1638 Dendroecological potential of *Callitris preissii* for dating historical fires in semi-arid shrublands  
1639 of southern Western Australia. *Dendrochronologia* 28, 37–48.  
1640 <https://doi.org/10.1016/j.dendro.2009.01.002>
- 1641 Orland, I.J., Burstyn, Y., Bar-Matthews, M., Kozdon, R., Ayalon, A., Matthews, A., Valley, J.W.,  
1642 2014. Seasonal climate signals (1990–2008) in a modern Soreq Cave stalagmite as revealed by  
1643 high-resolution geochemical analysis. *Chem. Geol.* 363, 322–333.  
1644 <https://doi.org/10.1016/j.chemgeo.2013.11.011>

- 1645 Orland, I.J., He, F., Bar-Matthews, M., Chen, G., Ayalon, A., Kutzbach, J.E., 2019. Resolving  
1646 seasonal rainfall changes in the Middle East during the last interglacial period. *Proc. Natl. Acad.*  
1647 *Sci.* 116, 24985–24990. <https://doi.org/10.1073/pnas.1903139116>
- 1648 Osborne, R.A.L., 1993. The History of Karstification at Wombeyan Caves, New South Wales,  
1649 Australia, as revealed by Palaeokarst Deposits. *Cave Sci.* 20, 1–8.
- 1650 Pearce, N.J.G., Perkins, W.T., Westgate, J.A., Gorton, M.P., Jackson, S.E., Neal, C.R., Chenery,  
1651 S.P., 1997. A Compilation of New and Published Major and Trace Element Data for NIST SRM  
1652 610 and NIST SRM 612 Glass Reference Materials. *Geostand. Newsl.* 21, 115–144.  
1653 <https://doi.org/10.1111/j.1751-908X.1997.tb00538.x>
- 1654 Pearson, A.R., Hartland, A., Frisia, S., Fox, B.R.S., 2020. Formation of calcite in the presence of  
1655 dissolved organic matter: Partitioning, fabrics and fluorescence. *Chem. Geol.* 539, 119492.  
1656 <https://doi.org/10.1016/j.chemgeo.2020.119492>
- 1657 Pechony, O., Shindell, D.T., 2010. Driving forces of global wildfires over the past millennium  
1658 and the forthcoming century. *Proc. Natl. Acad. Sci.* 107, 19167–19170.  
1659 <https://doi.org/10.1073/pnas.1003669107>
- 1660 Pereira, P., Úbeda, X., 2010. Spatial distribution of heavy metals released from ashes after a  
1661 wildfire. *J. Environ. Eng. Landsc. Manag.* 18, 13–22. <https://doi.org/10.3846/jeelm.2010.02>
- 1662 Peters, C., Church, M.J., Mitchell, C., 2001. Investigation of fire ash residues using mineral  
1663 magnetism. *Archaeol. Prospect.* 8, 227–237. <https://doi.org/10.1002/arp.171>
- 1664 Pharo, E.J., Meagher, D.A., Lindenmayer, D.B., 2013. Bryophyte persistence following major  
1665 fire in eucalypt forest of southern Australia. *For. Ecol. Manag.* 296, 24–32.  
1666 <https://doi.org/10.1016/j.foreco.2013.01.018>
- 1667 Power, M.J., Marlon, J., Ortiz, N., Bartlein, P.J., Harrison, S.P., Mayle, F.E., Ballouche, A.,  
1668 Bradshaw, R.H.W., Carcaillet, C., Cordova, C., Mooney, S., Moreno, P.I., Prentice, I.C.,  
1669 Thonicke, K., Tinner, W., Whitlock, C., Zhang, Y., Zhao, Y., Ali, A.A., Anderson, R.S., Beer, R.,  
1670 Behling, H., Briles, C., Brown, K.J., Brunelle, A., Bush, M., Camill, P., Chu, G.Q., Clark, J.,  
1671 Colombaroli, D., Connor, S., Daniau, A.-L., Daniels, M., Dodson, J., Doughty, E., Edwards, M.E.,  
1672 Finsinger, W., Foster, D., Frechette, J., Gaillard, M.-J., Gavin, D.G., Gobet, E., Haberle, S.,  
1673 Hallett, D.J., Higuera, P., Hope, G., Horn, S., Inoue, J., Kaltenrieder, P., Kennedy, L., Kong,  
1674 Z.C., Larsen, C., Long, C.J., Lynch, J., Lynch, E.A., McGlone, M., Meeks, S., Mensing, S., Meyer,  
1675 G., Minckley, T., Mohr, J., Nelson, D.M., New, J., Newnham, R., Noti, R., Oswald, W., Pierce, J.,  
1676 Richard, P.J.H., Rowe, C., Sanchez Goñi, M.F., Shuman, B.N., Takahara, H., Toney, J., Turney,  
1677 C., Urrego-Sanchez, D.H., Umbanhowar, C., Vandergoes, M., Vanniere, B., Vescovi, E., Walsh,  
1678 M., Wang, X., Williams, N., Wilmshurst, J., Zhang, J.H., 2008. Changes in fire regimes since the  
1679 Last Glacial Maximum: an assessment based on a global synthesis and analysis of charcoal data.  
1680 *Clim. Dyn.* 30, 887–907. <https://doi.org/10.1007/s00382-007-0334-x>

- 1681 Power, M.J., Marlon, J.R., Bartlein, P.J., Harrison, S.P., 2010. Fire history and the Global  
1682 Charcoal Database: A new tool for hypothesis testing and data exploration. *Palaeogeogr.*  
1683 *Palaeoclimatol. Palaeoecol.* 291, 52–59. <https://doi.org/10.1016/j.palaeo.2009.09.014>
- 1684 Ramsey, M.H., Potts, P.J., Webb, P.C., Watkins, P., Watson, J.S., Coles, B.J., 1995. An objective  
1685 assessment of analytical method precision: comparison of ICP-AES and XRF for the analysis of  
1686 silicate rocks. *Chem. Geol., Analytical Spectroscopy in the Earth Sciences* 124, 1–19.  
1687 [https://doi.org/10.1016/0009-2541\(95\)00020-M](https://doi.org/10.1016/0009-2541(95)00020-M)
- 1688 Rasbury, E.T., Cole, J.M., 2009. Directly dating geologic events: U-Pb dating of carbonates. *Rev.*  
1689 *Geophys.* 47. <https://doi.org/10.1029/2007RG000246>
- 1690 Read, P., Denniss, R., 2020. With costs approaching \$100 billion, the fires are Australia's  
1691 costliest natural disaster [WWW Document]. *The Conversation*. URL  
1692 [http://theconversation.com/with-costs-approaching-100-billion-the-fires-are-australias-](http://theconversation.com/with-costs-approaching-100-billion-the-fires-are-australias-costliest-natural-disaster-129433)  
1693 [costliest-natural-disaster-129433](http://theconversation.com/with-costs-approaching-100-billion-the-fires-are-australias-costliest-natural-disaster-129433) (accessed 6.29.21).
- 1694 Reale, J.K., Van Horn, D.J., Condon, K.E., Dahm, C.N., 2015. The effects of catastrophic wildfire  
1695 on water quality along a river continuum. *Freshw. Sci.* 34, 1426–1442.  
1696 <https://doi.org/10.1086/684001>
- 1697 Rehn, E., Rowe, C., Ulm, S., Woodward, C., Bird, M., 2021. A late-Holocene multiproxy fire  
1698 record from a tropical savanna, eastern Arnhem Land, Northern Territory, Australia. *The*  
1699 *Holocene* 31, 870–883. <https://doi.org/10.1177/0959683620988030>
- 1700 Reifsnyder, W.E., Herrington, L.P., Splat, K.W., 1967. Thermophysical Properties of Bark of  
1701 Shortleaf, Longleaf, and Red Pine. *Yale Sch. For. Environ. Stud. Bull. Ser.* 80.
- 1702 Richards, D.A., Bottrell, S.H., Cliff, R.A., Ströhle, K., Rowe, P.J., 1998. U-Pb dating of a  
1703 speleothem of Quaternary age. *Geochim. Cosmochim. Acta* 62, 3683–3688.  
1704 [https://doi.org/10.1016/S0016-7037\(98\)00256-7](https://doi.org/10.1016/S0016-7037(98)00256-7)
- 1705 Richardson, D., Black, A.S., Irving, D., Matear, R.J., Monselesan, D.P., Risbey, J.S., Squire, D.T.,  
1706 Tozer, C.R., 2022. Global increase in wildfire potential from compound fire weather and  
1707 drought. *Npj Clim. Atmospheric Sci.* 5, 23. <https://doi.org/10.1038/s41612-022-00248-4>
- 1708 Roy, D.P., Boschetti, L., Maier, S.W., Smith, A.M.S., 2010. Field estimation of ash and char  
1709 colour-lightness using a standard grey scale. *Int. J. Wildland Fire* 19, 698.  
1710 <https://doi.org/10.1071/WF09133>
- 1711 Rubino, M., D'Onofrio, A., Seki, O., Bendle, J.A., 2016. Ice-core records of biomass burning.  
1712 *Anthr. Rev.* 3, 140–162. <https://doi.org/10.1177/2053019615605117>
- 1713 Sander, M.-L., Andrén, O., 1997. Ash from Cereal and Rape Straw Used for Heat Production:  
1714 Liming Effect and Contents of Plant Nutrients and Heavy Metals. *Water. Air. Soil Pollut.* 93,  
1715 93–108. <https://doi.org/10.1023/A:1022179708289>

- Santín, C., Doerr, S.H., Shakesby, R.A., Bryant, R., Sheridan, G.J., Lane, P.N.J., Smith, H.G., Bell, T.L., 2012. Carbon loads, forms and sequestration potential within ash deposits produced by wildfire: new insights from the 2009 ‘Black Saturday’ fires, Australia. *Eur. J. For. Res.* 131, 1245–1253. <https://doi.org/10.1007/s10342-012-0595-8>
- Schmidt, G.A., Annan, J.D., Bartlein, P.J., Cook, B.I., Guilyardi, E., Hargreaves, J.C., Harrison, S.P., Kageyama, M., LeGrande, A.N., Konecky, B., Lovejoy, S., Mann, M.E., Masson-Delmotte, V., Risi, C., Thompson, D., Timmermann, A., Tremblay, L.-B., Yiou, P., 2014. Using palaeoclimate comparisons to constrain future projections in CMIP5. *Clim. Past* 10, 221–250. <https://doi.org/10.5194/cp-10-221-2014>
- Scroxton, N., Burns, S., Dawson, P., Rhodes, J.M., Brent, K., McGee, D., Heijnis, H., Gadd, P., Hantoro, W., Gagan, M., 2018. Rapid measurement of strontium in speleothems using core-scanning micro X-ray fluorescence. *Chem. Geol.* 487, 12–22. <https://doi.org/10.1016/j.chemgeo.2018.04.008>
- Šebela, S., Miler, M., Skobe, S., Torkar, S., Zupančič, N., 2015. Characterization of black deposits in karst caves, examples from Slovenia. *Facies* 61, 6. <https://doi.org/10.1007/s10347-015-0430-z>
- Šebela, S., Zupančič, N., Miler, M., Grčman, H., Jarc, S., 2017. Evidence of Holocene surface and near-surface palaeofires in karst caves and soils. *Palaeogeogr. Palaeoclimatol. Palaeoecol.* 485, 224–235. <https://doi.org/10.1016/j.palaeo.2017.06.015>
- Shakesby, R.A., 2011. Post-wildfire soil erosion in the Mediterranean: Review and future research directions. *Earth-Sci. Rev.* 105, 71–100. <https://doi.org/10.1016/j.earscirev.2011.01.001>
- Sherson, L.R., Van Horn, D.J., Gomez-Velez, J.D., Crossey, L.J., Dahm, C.N., 2015. Nutrient dynamics in an alpine headwater stream: use of continuous water quality sensors to examine responses to wildfire and precipitation events. *Hydrol. Process.* 29, 3193–3207. <https://doi.org/10.1002/hyp.10426>
- Sinclair, D.J., Kinsley, L.P.J., McCulloch, M.T., 1998. High resolution analysis of trace elements in corals by laser ablation ICP-MS. *Geochim. Cosmochim. Acta* 62, 1889–1901. [https://doi.org/10.1016/S0016-7037\(98\)00112-4](https://doi.org/10.1016/S0016-7037(98)00112-4)
- Sliwinski, J.T., Stoll, H.M., 2021. Combined fluorescence imaging and LA-ICP-MS trace element mapping of stalagmites: Microfabric identification and interpretation. *Chem. Geol.* 581, 120397. <https://doi.org/10.1016/j.chemgeo.2021.120397>
- Smith, C.L., Fairchild, I.J., Spötl, C., Frisia, S., Borsato, A., Moreton, S.G., Wynn, P.M., 2009. Chronology building using objective identification of annual signals in trace element profiles of stalagmites. *Quat. Geochronol.* 4, 11–21. <https://doi.org/10.1016/j.quageo.2008.06.005>

- Spate, A., Ward, J.K., 1979. A preliminary note on the black speleothems at Jersey Cave, Yarrangobilly, NSW, in: Proceedings of the 12th Conference of the Australian Speleological Federation. Presented at the 12th Conference of the Australian Speleological Federation, The Australian Speleological Federation, Perth.
- Spötl, C., Matthey, D., 2006. Stable isotope microsampling of speleothems for palaeoenvironmental studies: A comparison of microdrill, micromill and laser ablation techniques. *Chem. Geol.* 235, 48–58. <https://doi.org/10.1016/j.chemgeo.2006.06.003>
- Stamou, Z., Xystrakis, F., Koutsias, N., 2016. The role of fire as a long-term landscape modifier: Evidence from long-term fire observations (1922–2000) in Greece. *Appl. Geogr.* 74, 47–55. <https://doi.org/10.1016/j.apgeog.2016.07.005>
- Stronach, N.R.H., McNaughton, S.J., 1989. Grassland Fire Dynamics in the Serengeti Ecosystem, and a Potential Method of Retrospectively Estimating Fire Energy. *J. Appl. Ecol.* 26, 1025–1033. <https://doi.org/10.2307/2403709>
- Swetnam, T.W., Baisan, C.H., Caprio, A.C., Brown, P.M., Touchan, R., Anderson, R.S., Hallett, D.J., 2009. Multi-Millennial Fire History of the Giant Forest, Sequoia National Park, California, USA. *Fire Ecol.* 5, 120–150. <https://doi.org/10.4996/fireecology.0503120>
- Tan, L., Cai, Y., An, Z., Cheng, H., Shen, C.-C., Breitenbach, S.F.M., Gao, Y., Edwards, R.L., Zhang, H., Du, Y., 2015. A Chinese cave links climate change, social impacts and human adaptation over the last 500 years. *Sci. Rep.* 5, 12284. <https://doi.org/10.1038/srep12284>
- Teixeira, J.C., Folberth, G.A., O'Connor, F.M., Unger, N., Voulgarakis, A., 2021. Coupling interactive fire with atmospheric composition and climate in the UK Earth System Model. *Geosci. Model Dev.* 14, 6515–6539. <https://doi.org/10.5194/gmd-14-6515-2021>
- Thomas, Z.A., Mooney, S., Cadd, H., Baker, A., Turney, C., Schneider, L., Hogg, A., Haberle, S., Green, K., Weyrich, L.S., Pérez, V., Moore, N.E., Zawadzki, A., Kelloway, S.J., Khan, S.J., 2022. Late Holocene climate anomaly concurrent with fire activity and ecosystem shifts in the eastern Australian Highlands. *Sci. Total Environ.* 802, 149542. <https://doi.org/10.1016/j.scitotenv.2021.149542>
- Tibby, J., Tyler, J.J., Barr, C., 2018. Post little ice age drying of eastern Australia conflates understanding of early settlement impacts. *Quat. Sci. Rev.* 202, 45–52. <https://doi.org/10.1016/j.quascirev.2018.10.033>
- Treble, P., Shelley, J.M.G., Chappell, J., 2003. Comparison of high resolution sub-annual records of trace elements in a modern (1911–1992) speleothem with instrumental climate data from southwest Australia. *Earth Planet. Sci. Lett.* 216, 141–153. [https://doi.org/10.1016/S0012-821X\(03\)00504-1](https://doi.org/10.1016/S0012-821X(03)00504-1)

- 1785 Treble, P.C., Baker, A., Abram, N.J., Hellstrom, J.C., Crawford, J., Gagan, M.K., Borsato, A.,  
1786 Griffiths, A.D., Bajo, P., Markowska, M., Priestley, S.C., Hankin, S., Paterson, D., 2022.  
1787 Ubiquitous karst hydrological control on speleothem oxygen isotope variability in a global study.  
1788 *Commun. Earth Environ.* 3, 1–10. <https://doi.org/10.1038/s43247-022-00347-3>
- 1789 Treble, P.C., Baker, A., Ayliffe, L.K., Cohen, T.J., Hellstrom, J.C., Gagan, M.K., Frisia, S.,  
1790 Drysdale, R.N., Griffiths, A.D., Borsato, A., 2017. Hydroclimate of the Last Glacial Maximum  
1791 and deglaciation in southern Australia's arid margin interpreted from speleothem records (23–  
1792 15 ka). *Clim. Past* 13, 667–687. <https://doi.org/10.5194/cp-13-667-2017>
- 1793 Treble, P.C., Chappell, J., Shelley, J.M.G., 2005. Complex speleothem growth processes revealed  
1794 by trace element mapping and scanning electron microscopy of annual layers. *Geochim.*  
1795 *Cosmochim. Acta* 69, 4855–4863. <https://doi.org/10.1016/j.gca.2005.06.008>
- 1796 Treble, P.C., Fairchild, I.J., Baker, A., Meredith, K.T., Andersen, M.S., Salmon, S.U., Bradley, C.,  
1797 Wynn, P.M., Hankin, S.I., Wood, A., McGuire, E., 2016. Roles of forest bioproductivity,  
1798 transpiration and fire in a nine-year record of cave dripwater chemistry from southwest  
1799 Australia. *Geochim. Cosmochim. Acta* 184, 132–150.  
1800 <https://doi.org/10.1016/j.gca.2016.04.017>
- 1801 Tuhý, M., Ettler, V., Rohovec, J., Matoušková, Š., Mihaljevič, M., Kříbek, B., Mapani, B., 2021.  
1802 Metal(loid)s remobilization and mineralogical transformations in smelter-polluted savanna soils  
1803 under simulated wildfire conditions. *J. Environ. Manage.* 293, 112899.  
1804 <https://doi.org/10.1016/j.jenvman.2021.112899>
- 1805 Urban, T.M., Rasic, J.T., Alix, C., Anderson, D.D., Chisholm, L., Jacob, R.W., Manning, S.W.,  
1806 Mason, O.K., Tremayne, A.H., Vinson, D., 2019. Magnetic detection of archaeological hearths in  
1807 Alaska: A tool for investigating the full span of human presence at the gateway to North  
1808 America. *Quat. Sci. Rev.* 211, 73–92. <https://doi.org/10.1016/j.quascirev.2019.03.018>
- 1809 Uribe, C., Inclán, R., Sánchez, D.M., Clavero, M.A., Fernández, A.M., Morante, R., Cardena, A.,  
1810 Blanco, A., Van Miegroet, H., 2013. Effect of wildfires on soil respiration in three typical  
1811 Mediterranean forest ecosystems in Madrid, Spain. *Plant Soil* 369, 403–420.  
1812 <https://doi.org/10.1007/s11104-012-1576-x>
- 1813 Vachula, R.S., Huang, Y., Longo, W.M., Dee, S.G., Daniels, W.C., Russell, J.M., 2019. Evidence  
1814 of Ice Age humans in eastern Beringia suggests early migration to North America. *Quat. Sci.*  
1815 *Rev.* 205, 35–44. <https://doi.org/10.1016/j.quascirev.2018.12.003>
- 1816 Vachula, R.S., Karp, A.T., Denis, E.H., Balascio, N.L., Canuel, E.A., Huang, Y., 2022. Spatially  
1817 calibrating polycyclic aromatic hydrocarbons (PAHs) as proxies of area burned by vegetation  
1818 fires: Insights from comparisons of historical data and sedimentary PAH fluxes. *Palaeogeogr.*  
1819 *Palaeoclimatol. Palaeoecol.* 596, 110995. <https://doi.org/10.1016/j.palaeo.2022.110995>

- 1820 Vachula, R.S., Russell, J.M., Huang, Y., Richter, N., 2018. Assessing the spatial fidelity of  
 1821 sedimentary charcoal size fractions as fire history proxies with a high-resolution sediment  
 1822 record and historical data. *Palaeogeogr. Palaeoclimatol. Palaeoecol.* 508, 166–175.  
 1823 <https://doi.org/10.1016/j.palaeo.2018.07.032>
- 1824 van Beynen, P., Bourbonniere, R., Ford, D., Schwarcz, H., 2001. Causes of colour and  
 1825 fluorescence in speleothems. *Chem. Geol.* 175, 319–341. [https://doi.org/10.1016/S0009-](https://doi.org/10.1016/S0009-2541(00)00343-0)  
 1826 [2541\(00\)00343-0](https://doi.org/10.1016/S0009-2541(00)00343-0)
- 1827 van Etten, E.J.B., Davis, R.A., Doherty, T.S., 2021. Fire in Semi-Arid Shrublands and  
 1828 Woodlands: Spatial and Temporal Patterns in an Australian Landscape. *Front. Ecol. Evol.* 9,  
 1829 382. <https://doi.org/10.3389/fevo.2021.653870>
- 1830 van Marle, M.J.E., Kloster, S., Magi, B.I., Marlon, J.R., Daniau, A.-L., Field, R.D., Arneth, A.,  
 1831 Forrest, M., Hantson, S., Kehrwald, N.M., Knorr, W., Lasslop, G., Li, F., Mangeon, S., Yue, C.,  
 1832 Kaiser, J.W., van der Werf, G.R., 2017. Historic global biomass burning emissions for CMIP6  
 1833 (BB4CMIP) based on merging satellite observations with proxies and fire models (1750–2015).  
 1834 *Geosci. Model Dev.* 10, 3329–3357. <https://doi.org/10.5194/gmd-10-3329-2017>
- 1835 Wang, C., Bendle, J.A., Greene, S.E., Griffiths, M.L., Huang, J., Moossen, H., Zhang, H., Ashley,  
 1836 K., Xie, S., 2019. Speleothem biomarker evidence for a negative terrestrial feedback on climate  
 1837 during Holocene warm periods. *Earth Planet. Sci. Lett.* 525, 115754.  
 1838 <https://doi.org/10.1016/j.epsl.2019.115754>
- 1839 Wang, D., Guan, D., Zhu, S., Kinnon, M.M., Geng, G., Zhang, Q., Zheng, H., Lei, T., Shao, S.,  
 1840 Gong, P., Davis, S.J., 2021. Economic footprint of California wildfires in 2018. *Nat. Sustain.* 4,  
 1841 252–260. <https://doi.org/10.1038/s41893-020-00646-7>
- 1842 Wang, H., Treble, P., Baker, A., Rich, A.M., Bhattacharyya, S., Oriani, F., Akter, R., Chinu, K.,  
 1843 Wainwright, I., Marjo, C.E., 2022. Sulphur variations in annually layered stalagmites using  
 1844 benchtop micro-XRF. *Spectrochim. Acta Part B At. Spectrosc.* 189, 106366.  
 1845 <https://doi.org/10.1016/j.sab.2022.106366>
- 1846 Wang, X., Xiao, J., Cui, L., Ding, Z., 2013. Holocene changes in fire frequency in the Daihai Lake  
 1847 region (north-central China): indications and implications for an important role of human  
 1848 activity. *Quat. Sci. Rev.* 59, 18–29. <https://doi.org/10.1016/j.quascirev.2012.10.033>
- 1849 Ward, M., Tulloch, A.I.T., Radford, J.Q., Williams, B.A., Reside, A.E., Macdonald, S.L., Mayfield,  
 1850 H.J., Maron, M., Possingham, H.P., Vine, S.J., O'Connor, J.L., Massingham, E.J., Greenville,  
 1851 A.C., Woinarski, J.C.Z., Garnett, S.T., Lintermans, M., Scheele, B.C., Carwardine, J., Nimmo,  
 1852 D.G., Lindenmayer, D.B., Kooyman, R.M., Simmonds, J.S., Sonter, L.J., Watson, J.E.M., 2020.  
 1853 Impact of 2019–2020 mega-fires on Australian fauna habitat. *Nat. Ecol. Evol.* 4, 1321–1326.  
 1854 <https://doi.org/10.1038/s41559-020-1251-1>

- 1855 Webb, M., Dredge, J., Barker, P.A., Müller, W., Jex, C., Desmarchelier, J., Hellstrom, J., Wynn,  
1856 P.M., 2014. Quaternary climatic instability in south-east Australia from a multi-proxy  
1857 speleothem record. *J. Quat. Sci.* 29, 589–596. <https://doi.org/10.1002/jqs.2734>
- 1858 Whitlock, C., Larsen, C., 2001. Charcoal as a Fire Proxy, in: Smol, J.P., Birks, H.J.B., Last, W.M.,  
1859 Bradley, R.S., Alverson, K. (Eds.), *Tracking Environmental Change Using Lake Sediments:*  
1860 *Terrestrial, Algal, and Siliceous Indicators, Developments in Paleoenvironmental Research.*  
1861 Springer Netherlands, Dordrecht, pp. 75–97. [https://doi.org/10.1007/0-306-47668-1\\_5](https://doi.org/10.1007/0-306-47668-1_5)
- 1862 Woodhead, J., Hellstrom, J., Maas, R., Drysdale, R., Zanchetta, G., Devine, P., Taylor, E., 2006.  
1863 U–Pb geochronology of speleothems by MC-ICPMS. *Quat. Geochronol.* 1, 208–221.  
1864 <https://doi.org/10.1016/j.quageo.2006.08.002>
- 1865 Woodhead, J.D., Hellstrom, J., Hergt, J.M., Greig, A., Maas, R., 2007. Isotopic and Elemental  
1866 Imaging of Geological Materials by Laser Ablation Inductively Coupled Plasma-Mass  
1867 Spectrometry. *Geostand. Geoanalytical Res.* 31, 331–343. [https://doi.org/10.1111/j.1751-](https://doi.org/10.1111/j.1751-908X.2007.00104.x)  
1868 [908X.2007.00104.x](https://doi.org/10.1111/j.1751-908X.2007.00104.x)
- 1869 Woods, S.W., Balfour, V.N., 2010. The effects of soil texture and ash thickness on the post-fire  
1870 hydrological response from ash-covered soils. *J. Hydrol.* 393, 274–286.  
1871 <https://doi.org/10.1016/j.jhydrol.2010.08.025>
- 1872 Wu, G., Wang, D.Y., 2012. Mechanical and Acoustic Emission Characteristics of Limestone after  
1873 High Temperature. *Adv. Mater. Res.* 446–449, 23–28.  
1874 <https://doi.org/10.4028/www.scientific.net/AMR.446-449.23>
- 1875 Wu, J.Y., Wang, Y.J., Cheng, H., Kong, X.G., Liu, D.B., 2012. Stable isotope and trace element  
1876 investigation of two contemporaneous annually-laminated stalagmites from northeastern China  
1877 surrounding the “8.2 ka event”; *Clim. Past* 8, 1497–1507.  
1878 <https://doi.org/10.5194/cp-8-1497-2012>
- 1879 Wynn, P.M., Borsato, A., Baker, A., Frisia, S., Miorandi, R., Fairchild, I.J., 2013. Biogeochemical  
1880 cycling of sulphur in karst and transfer into speleothem archives at Grotta di Ernesto, Italy.  
1881 *Biogeochemistry* 114, 255–267. <https://doi.org/10.1007/s10533-012-9807-z>
- 1882 Wynn, P.M., Brocks, J.J., 2014. A framework for the extraction and interpretation of organic  
1883 molecules in speleothem carbonate. *Rapid Commun. Mass Spectrom.* 28, 845–854.  
1884 <https://doi.org/10.1002/rcm.6843>
- 1885 Wynn, P.M., Fairchild, I.J., Baker, A., Baldini, J.U.L., McDermott, F., 2008. Isotopic archives of  
1886 sulphate in speleothems. *Geochim. Cosmochim. Acta* 72, 2465–2477.  
1887 <https://doi.org/10.1016/j.gca.2008.03.002>
- 1888 Wynn, P.M., Fairchild, I.J., Borsato, A., Spötl, C., Hartland, A., Baker, A., Frisia, S., Baldini,  
1889 J.U.L., 2018. Sulphate partitioning into calcite: Experimental verification of pH control and



- 1890 application to seasonality in speleothems. *Geochim. Cosmochim. Acta* 226, 69–83.
- 1891 <https://doi.org/10.1016/j.gca.2018.01.020>
- 1892 Wynn, P.M., Fairchild, I.J., Frisia, S., Spötl, C., Baker, A., Borsato, A., 2010. High-resolution
- 1893 sulphur isotope analysis of speleothem carbonate by secondary ionisation mass spectrometry.
- 1894 *Chem. Geol.* 271, 101–107. <https://doi.org/10.1016/j.chemgeo.2010.01.001>
- 1895 Wynn, P.M., Fairchild, I.J., Spötl, C., Hartland, A., Matthey, D., Fayard, B., Cotte, M., 2014.
- 1896 Synchrotron X-ray distinction of seasonal hydrological and temperature patterns in speleothem
- 1897 carbonate. *Environ. Chem.* 11, 28. <https://doi.org/10.1071/EN13082>
- 1898 Wynn, P.M., Morrell, D.J., Tuffen, H., Barker, P., Tweed, F.S., Burns, R., 2015. Seasonal release
- 1899 of anoxic geothermal meltwater from the Katla volcanic system at Sólheimajökull, Iceland.
- 1900 *Chem. Geol.* 396, 228–238. <https://doi.org/10.1016/j.chemgeo.2014.12.026>
- 1901 Zedler, P.H., 2007. Fire Effects on Grasslands, in: Johnson, E.A., Miyanishi, K. (Eds.), *Plant*
- 1902 *Disturbance Ecology*. Academic Press, Burlington, pp. 397–439. [https://doi.org/10.1016/B978-](https://doi.org/10.1016/B978-012088778-1/50015-7)
- 1903 [012088778-1/50015-7](https://doi.org/10.1016/B978-012088778-1/50015-7)
- 1904 Zennaro, P., Kehrwald, N., Marlon, J., Ruddiman, W.F., Brücher, T., Agostinelli, C., Dahl-
- 1905 Jensen, D., Zangrando, R., Gambaro, A., Barbante, C., 2015. Europe on fire three thousand
- 1906 years ago: Arson or climate? *Geophys. Res. Lett.* 42, 5023–2033.
- 1907 <https://doi.org/10.1002/2015GL064259>
- 1908 Zhao, J., Yu, K., Feng, Y., 2009. High-precision  $^{238}\text{U}$ – $^{234}\text{U}$ – $^{230}\text{Th}$  disequilibrium dating of
- 1909 the recent past: a review. *Quat. Geochronol.* 4, 423–433.
- 1910 <https://doi.org/10.1016/j.quageo.2009.01.012>
- 1911 Zupančič, N., Šebela, S., Miler, M., 2011. Mineralogical and chemical characteristics of black
- 1912 coatings in Postojna cave system. *Acta Carsologica* 40. <https://doi.org/10.3986/ac.v40i2.15>